NGR-38-003-036

GRAPHICAL EVALUATION OF RELATIVISTIC MATRIX ELEMENTS

Keh-Ning Huang

Behlen Laboratory of Physics

The University of Nebraska

Lincoln, Nebraska 68588

(NASA-CR-155774) GRAPHICAL EVALUATION OF RELATIVISTIC MATRIX ELEMENTS (Nebraska Univ.) 83 p HC A05/MF A01 CSCL 20H

N78-18884

Unclas

G3/72 06569

See p 59 for acknowledgment of NASA support.

ABSTRACT

A graphical representation of angular momentum is used to evaluate relativistic matrix elements between antisymmetrized states of many-particle configurations having any number of open shells. The antisymmetrized matrix element is expanded as a sum of semisymmetrized matrix elements, which can be evaluated expediently in terms of radial integrals from easily constructed diagrams. The diagram representing a semisymmetrized matrix element is composed of four diagram blocks, namely, the bra block, the ket block, the spectator block, and the interaction block. The first three blocks indicate the couplings of the two interacting configurations while the last depends on the interaction and is the replaceable component. Interaction blocks for relativistic operators and commonly used potentials are summarized in ready-to-use forms. A simple step-by-step procedure is prescribed generally for calculating antisymmetrized matrix elements of one- and two-particle operators. A modified covariant 3-jm coefficient is also introduced along with certain new graphical notations. Although we focus on jj-coupled states, which comes naturally in a relativistic formulation, the general procedure holds in any coupling scheme.

CONTENTS

I. INTRODUCTION

A relativistic treatment including quantum-electrodynamic corrections has become essential in many fields of atomic physics; this requires the evaluation of matrix elements with considerable complexity. In particular, the possibility of forming highly ionized heavy atoms and the study of their structure and of their collision and subsequent cascade processes necessitate a complete treatment of couplings between several open shells. On the other hand, the application of Wigner-Racah's idea in these problems with standard techniques of angular-momentum coupling becomes a tedious and more often arduous task. The purpose of this work is to provide non-specialists with a simple and powerful tool to express complicated matrix elements in terms of radial integrals, suitable for numerical computation.

One of the essential approximations in the quantum-mechanical description of a many-particle system is the central field approximation. Orbitals of the particles can thus be represented by angular-momentum eigenstates. The coupling of angular-momentum eigenstates with irreducible tensor operators depend only on the rotational properties of the states and operators involved. This fact leads naturally to the division of the calculation of a physical quantity into two parts: One consists of dynamical variables invariant under rotations, and the other is a geometrical factor depending on the rotational properties of the physical quantity. It is the Wigner-Eckart theorem (Wigner, 1927; Eckart, 1930) which embodies this notion. The geometrical factor is given by the Clebsch-Gordan coefficient (also called the Wigner or vector-coupling coefficient) or by a more symmetric quantity, the Wigner 3-j coefficient (Wigner, 1951; Edmonds, 1957). Techniques for the solution of related algebraic problems for many-particle systems have been developed by Racah (1942a, 1942b, 1943). [Two other equally applicable approaches have been described in the works of Condon and Shortley (1935) and Harter and Patterson (1976), respectively, but will not be discussed here.] However, the complicated algebraic manipulations have prevented nonspecialists from carrying out specific calculations.

Attempts to solve the complexity of angular-momentum couplings result in graphical methods. In the early stage, angular-momentum diagrams were used only in a qualitative and descriptive way (see, e.g., Edmonds, 1957 and Judd, 1963). It was the achievement of Jucys, Levinson, and Vanagas (1962) that a graphical method was put on a quantitative basis so that angular-momentum couplings can be solved in an expedient and elegant manner solely in terms of diagrams. The graphical method of Jucys et al. starts by assigning a graphical symbol to the Wigner 3-j coefficient and compounds the angular-momentum coupling to 3n-j symbols. An alternative method given by Danos (1971) however focuses on the recoupling aspect and uses the 9-j recoupling as the central graphical element. The former has been particularly effective in extending the range of application of Racah's techniques. The graphical approach permits transformations on diagrammatic expressions and leads on to analytical results in a clear and simple manner. Besides its utility as a calculational tool, the graphical method has the appealing feature of revealing, at a glance, the structure of very complicated couplings of angular momenta. In addition, we do gain in the graphical form some physical insight, similar to the visual understanding of physical processes provided by Feynman diagrams. In fact, because of the role which the graphical method plays in extracting the geometrical part of a Feynman diagram (Bolotin, Levinson, and Tolmacher, 1964; Judd, 1967; El-Baz and

Nahabetian, 1969), it becomes an indispensable supplement to the Feynman diagrams, where a perturbed quantum mechanical system is studied graphically.

The graphical method has been developed subsequently by Jucys and Bandzaitis (1967), Massot, El-Baz, and Lafoucrière (1967), Brink and Satchler (1968), El-Baz (1969), Bordarier (1970), Briggs (1971), El-Baz and Castel (1971, 1972). El-Baz and co-workers have in particular extended the graphical method to treat spherical harmonics, irreducible tensor operators, and rotation matrices. The basic idea of El-Baz and Castel (1972) consists in representing graphically the bra (covariant) and ket (contravariant) vectors familiar in the Dirac notations (Dirac, 1930). The graphical representation of the Clebsh-Gordan coefficient thus becomes a straightforward extension of the bra and ket diagrams. The graphical representation of the Wigner 3-j coefficient, first introduced by Jucys et al. (1962), has been modified by El-Baz (1969) to better represent its covariant property, using Wigner's covariant notation (Wigner, 1959). We will adopt this idea of El-Baz with a modified phase factor to have a more coherent correspondence between the Wigner 3-j coefficient and the Clebsch-Gordan coefficient.

A graphical treatment of antisymmetrization for the evaluation of antisymmetrized matrix elements has been given by Bordarier (1970) and Briggs (1971). The Bordarier's treatment is general and encompasses many different types of matrix elements, while Briggs gives a step-by-step procedure for the evaluation of matrix elements between antisymmetrized states with LS coupling. An alternative treatment has been given by Huang and Starace (1978) for a particular case. The procedure of Bordarier and Briggs is however a little intricate between purely graphical steps and manipulations which are better to be performed analytically. For example, the antisym-

... different subshells may be carried out analytically with ease without resorting to a graphical phase rule. Furthermore, the interaction diagram is obtained in the Briggs' prescription by expanding the interaction operator in a complete set of particle orbitals, whereas a similar interaction diagram may be obtained by considering directly the m-scheme matrix element.

In this work, we will prescribe a simple step-by-step procedure for evaluating antisymmetrized matrix elements for one- and two-particle operators. Although we focus on jj-coupled states, which comes naturally in a relativistic formulation, the general procedure holds in any coupling scheme. The underlying idea of the present approach is to express analytically the matrix element between antisymmetrized many-particle states in terms of matrix elements between semisymmetrized many-particle states. The semisymmetrized many-particle state is defined as the many-particle state which is antisymmetric within each subshell but is not antisymmetric with respect to exchange of two particles from different subshells. Henceforth, the matrix elements between semisymmetrized many-particle states are evaluated by a graphical procedure. The graphical procedure consists of three major steps: Firstly, we construct diagrams for the two interacting semisymmetrized many-particle states and decouple active particles from the other particles to be referred to as the spectator particles. Here the active particles represent the typical particles which actually participate in the interaction in a semisymmetrized matrix element. Secondly, we insert the interaction block corresponding to the interaction between active particles. The interaction blocks for commonly used operators and potentials are summarized in ready-to-use forms in Appendix B. Lastly, we evaluate the resultant diagram by transforming it into basic diagrams representing 3n-j symbols, whose analytical values have been tabulated extensively (Rotenberg et al., 1959; Jucys et al., 1962). Thus the antisymmetrized matrix element is expressed as a sum of weighted radial integrals.

The graphical notation and transformation rules used in this work are given in Sec. II. The covariant 3-jm coefficient is defined there. In Sec. III an analytical procedure is outlined for evaluating the antisymmetrized matrix element in terms of radial integrals. In Sec. IV we describe in detail how the diagram representing the semisymmetrized matrix element can be constructed and evaluated. In Sec. V we summarize the procedure of evaluating antisymmetrized matrix elements. A worked example is given in Sec. VI. Appendix A is a glossary of definitions of terms used in this work; in most cases they are identified in the text by italic letters when they first appear. Graphical forms of commonly used operators and potentials are summarized in Appendix B. Appendix C gives the derivation of one of the expansion formulas used in Appendix B.

II. GRAPHICAL NOTATION AND TRANSFORMATION RULES

We will first define the basic coupling coefficient, i.e., the covariant 3-jm coefficient, and its graphical representation in Sec. II.A. Rules to combine 3-jm diagrams, which amount to summations over magnetic quantum numbers m, and rules to transform the combined diagram will be given in Sec. II.B. Section II.C summarizes analytical values of some basic diagrams. The graphical representation of the Clebsch-Gordan coefficient and its transformation to the 3-jm diagram is described in Sec. II.D. These find uses in constructing configuration diagrams.

A. The Covariant 3-jm Coefficient

Wigner's 3-j symbol is defined by

$$\begin{pmatrix} j_1 & j_2 & j_3 \\ m_1 & m_2 & -m_3 \end{pmatrix} = (-)^{j_1 - j_2 + m_3} (2j_3+1)^{-1/2} \langle j_1 m_1 j_2 m_2 | j_3 m_3 \rangle , \tag{2.1}$$

where $\langle j_1 m_1 j_2 m_2 | j_3 m_3 \rangle$ is the Clebsch-Gordan coefficient. We employ, however, the covariant notation (Wigner, 1959) such that <u>the covariant 3-jm coefficient</u> (or, simply, the 3-jm coefficient) which is covariant in the first two indices and contravariant in the last index is defined by

$$\begin{pmatrix} j_1 & j_2 & m_3 \\ m_1 & m_2 & j_3 \end{pmatrix} = (-)^{j_3 + m_3} \begin{pmatrix} j_1 & j_2 & j_3 \\ m_1 & m_2 & -m_3 \end{pmatrix}$$

$$= (-)^{j_1 - j_2 - j_3} (2j_3+1)^{-1/2} \langle j_1 m_1 j_2 m_2 | j_3 m_3 \rangle . \tag{2.2}$$

Note that this definition is different from Wigner's definition (Wigner, 1959) in that he used the phase factor $(-)^{j_3-m_3}$. This is also different from the definition of El-Baz and Castel (1972) in that our contravariant component is defined with the same phase as their covariant component. This modification, however, does not change the graphical rules presented in their work. We also emphasize that this coefficient is called "the covariant 3-jm coefficient" because of their covariance properties and m-dependence. Accordingly the name "3-j symbol" or "3-j coefficient" will be reserved for the coefficient occurring in the hierarchy of 3n-j coefficients, which have no m-dependence.

By our definition, the ordinary 3-j coefficient of Wigner is a fully covariant 3-jm coefficient and is equivalent to the fully contravariant 3-jm coefficient

$$\begin{pmatrix} m_1 & m_2 & m_3 \\ j_1 & j_2 & j_3 \end{pmatrix} = \begin{pmatrix} j_1 & j_2 & j_3 \\ m_1 & m_2 & m_3 \end{pmatrix}. \tag{2.3}$$

Note however that

$$\begin{pmatrix} j_1 & j_2 & m_3 \\ m_1 & m_2 & j_3 \end{pmatrix} = (-)^{2j_3} \begin{pmatrix} m_1 & m_2 & j_3 \\ j_1 & j_2 & m_3 \end{pmatrix}. \tag{2.4}$$

Graphically we can present a covariant 3-jm coefficient as

$$\begin{pmatrix} j_1 & j_2 & m_3 \\ m_1 & m_2 & j_3 \end{pmatrix} = \tag{2.5}$$

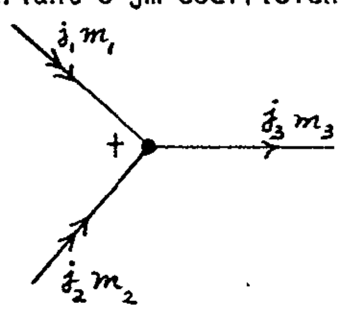

The notational rules are as follows:

(i) Each vertex, indicated by a node, represents a 3-jm coefficient. Each covariant component is denoted by a line with an ingoing double-arrow, and each contravariant component by a line with an outgoing single-arrow.

(ii) The plus (minus) sign at the node means that the angular momenta are to be read counterclockwise (clockwise). The change of the sign at the node $(j_1 j_2 j_3)$ introduces a phase factor $(-)^{j_1+j_2+j_3}$; therefore, the sign at the node may be suppressed if $(j_1+j_2+j_3)$ is an even number.

The magnetic quantum number of each angular momentum line is usually suppressed where no confusion may occur. Also, we note that the "current" of magnetic quantum numbers is conserved at each node due to the selection rule for magnetic quantum numbers of the covariant 3-jm coefficient; for example,

$$\begin{pmatrix} j_1 & j_2 & m_1+m_2 \\ m_1 & m_2 & j_3 \end{pmatrix} =$$

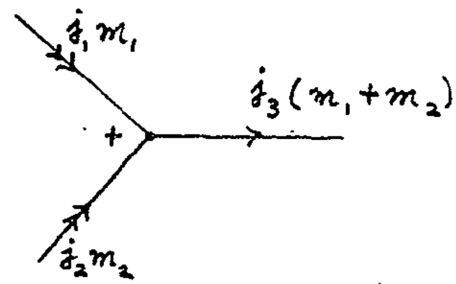

, (2.6)

where we have the sum of the ingoing currents "m_1" + "m_2" = the outgoing current "$m_1 + m_2$."

The notational rules used to combine 3-jm diagrams are as follows:

(i) The summation, or in the tensorial terms "contraction," over a pair of magnetic quantum numbers (one of which is always contravariant, and the other covariant) is performed by joining the corresponding angular-momentum lines to form a linked single-arrowed line.

(ii) The change in direction of a linked angular-momentum line j introduces a phase factor $(-)^{2j}$. As a result, we may suppress the arrow of a linked angular-momentum line j whenever j is an integer.

Although we do not write the magnetic quantum number for a linked angular-momentum line, the summation over the magnetic quantum number is always implied. Nevertheless, in many cases because of the conservation of the "magnetic current," the summation implied by a linked angular-momentum line exists only formally.

B. Transformation Rules for 3-jm Diagrams

There are only two fundamental transformation rules:

Rule I:

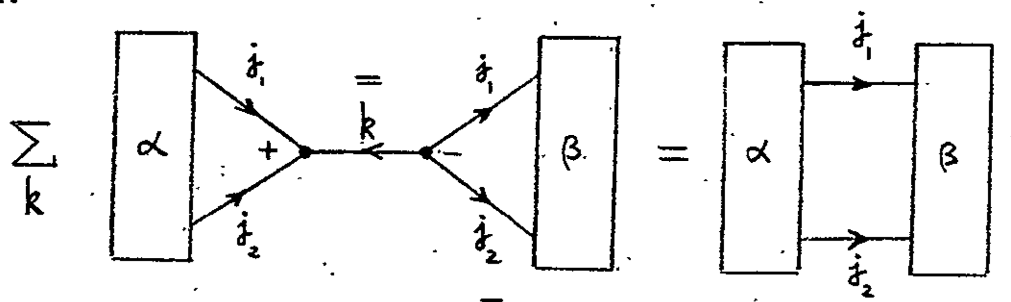

(2.7)

where a bar on the angular momentum $\bar{k}$ stands for a multiplication factor $(2k+1)^{1/2}$, and multiple bars for multiple factors. For example, $\bar{\bar{k}}$ indicates a factor (2k+1). Rule I follows from the graphical relation for 3-jm coefficients,

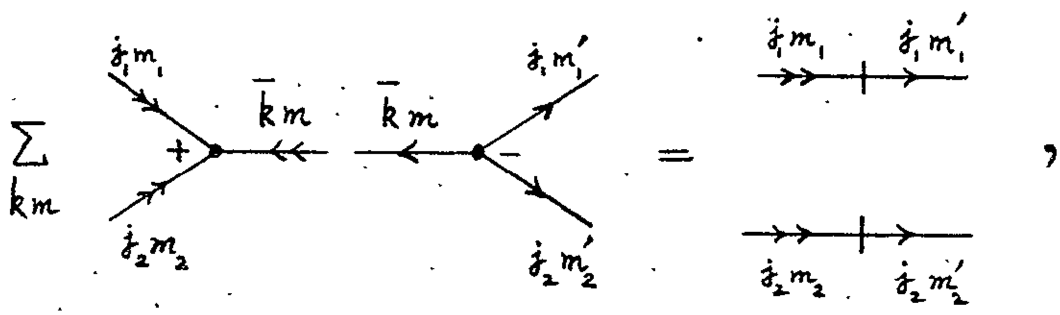

(2.8)

which represents the orthogonality relation

$$\sum_{km} (2k+1) \begin{pmatrix} j_1 & j_2 & k \\ m_1 & m_2 & m \end{pmatrix} \begin{pmatrix} m_1' & m_2' & m \\ j_1 & j_2 & k \end{pmatrix} = \delta_{m_1 m_1'} \, \delta_{m_2 m_2'} \, . \tag{2.9}$$

In (2.7) we use the blocks α and β to represent arbitrary diagrams either open or closed. By <u>open</u> or <u>closed</u>, we mean that the diagram either has or hasn't any free nonzero angular-momentum lines. For example, in the following diagram

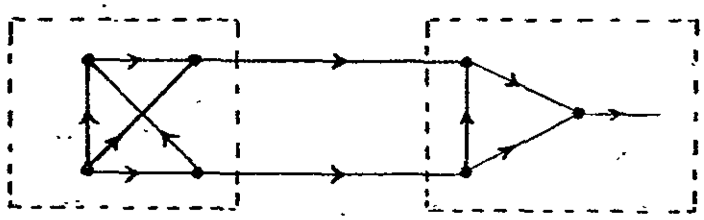

the diagram block on the left is closed while the one on the right open. We will use an encircled greek letter ⓐ to indicate specifically a closed diagram block.

Rule II:

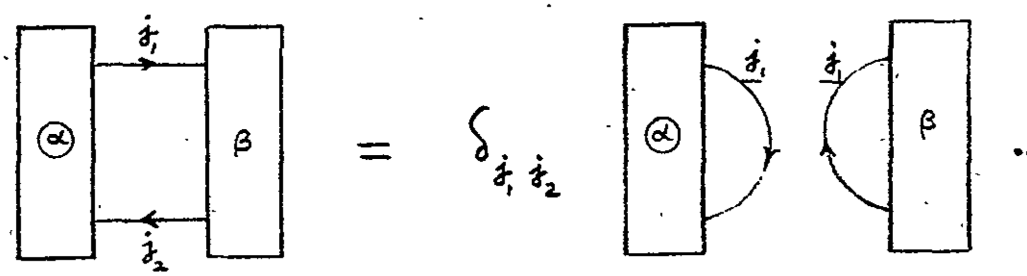

(2.10)

where the bar under the angular momentum $\underline{j_1}$ denotes a multiplication factor $(2j_1+1)^{-\frac{1}{2}}$. Also we will use multiple bars to indicate multiple factors. Since derivation of this transformation rule is more involved, we refer the reader to the works of Jucys et al. (1962) and El-Baz and Castel (1972) for its proof. Note that for a null block β, Rule II becomes

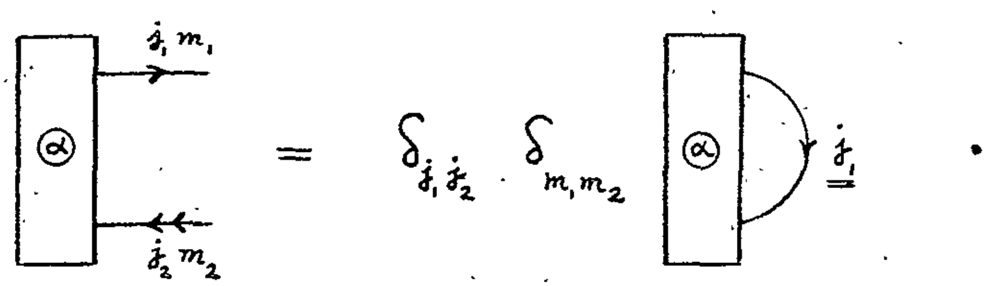

(2.11)

This transformation rule results from the rotational invariance of the diagram.

From these two fundamental rules, we can easily derive besides others the following additional useful rules:

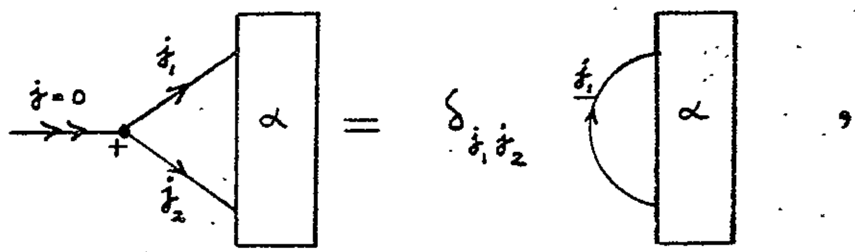

(2.12)

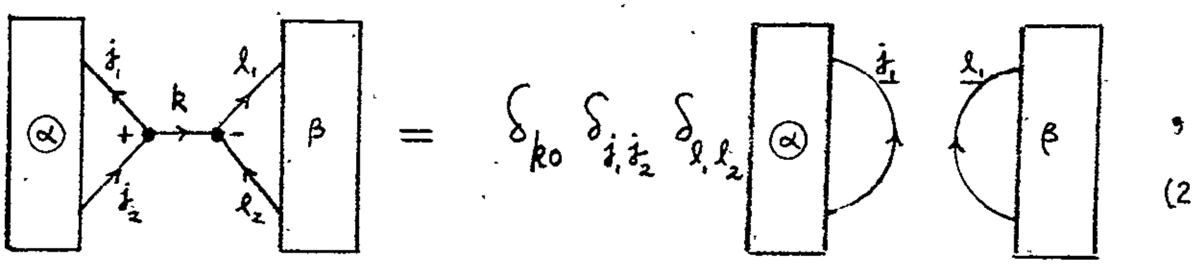

(2.13)

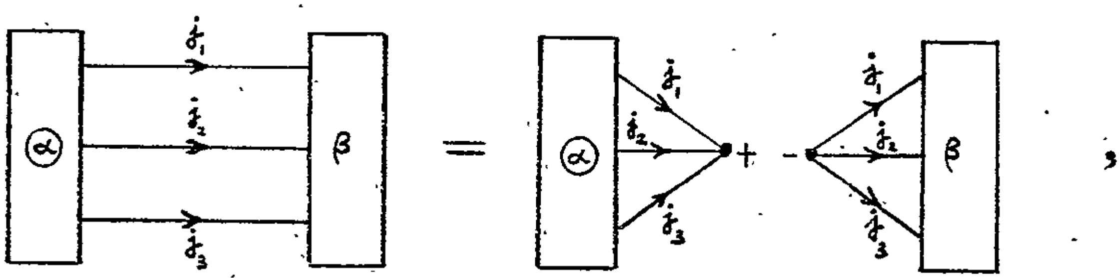

(2.14)

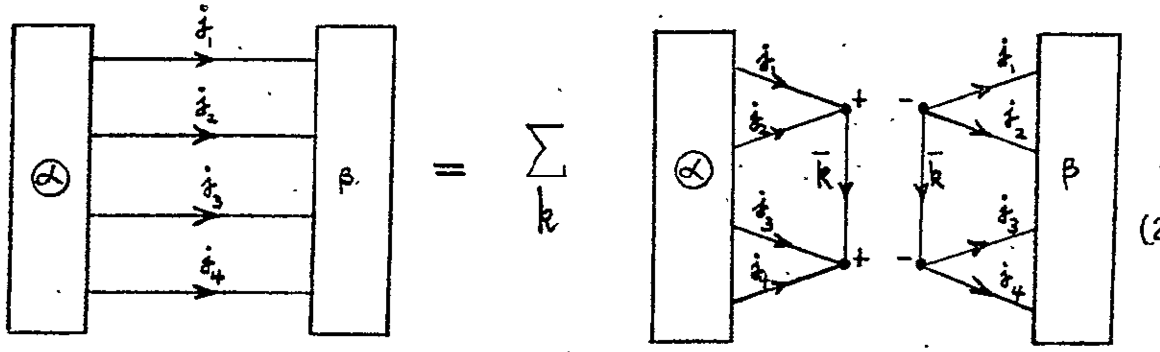

(2.15)

The transformation rules I and II and the rules derived from them allow one to rearrange diagrams or to factor out basic diagrams whose analytical values have been tabulated. Some of those basic diagrams are presented in the next subsection.

C. Analytical Values of Some Basic Diagrams

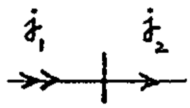

$$= (j_1 m_1 | j_2 m_2) = \delta_{j_1 j_2} \; \delta_{m_1 m_2} \, , \tag{2.16}$$

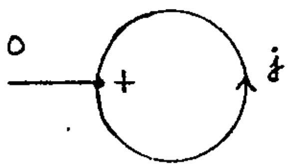

$$= (2j+1)^{1/2} \, , \tag{2.17}$$

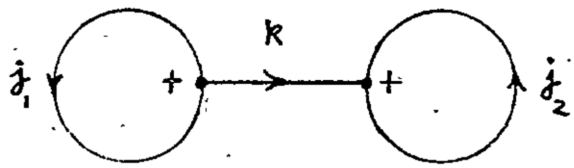

$$= \delta_{k0} (2j_1+1)^{1/2} (2j_2+1)^{1/2} \, , \tag{2.18}$$

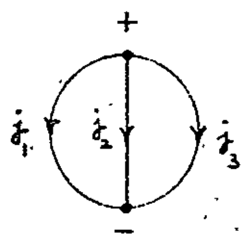

$$= \{ j_1 \; j_2 \; j_3 \} \, , \quad 3\text{-}j \text{ symbol}$$

$$= \begin{cases} 1 & \text{if } |j_1 - j_2| \leq j_3 \leq (j_1 + j_2), \\ 0 & \text{otherwise}, \end{cases} \tag{2.19}$$

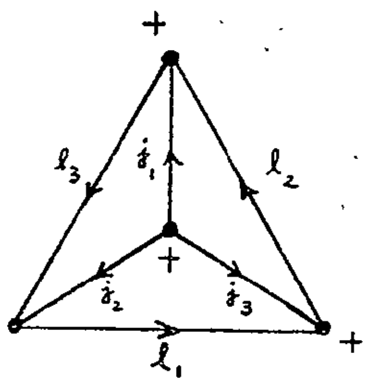

$$= \begin{Bmatrix} j_1 & j_2 & j_3 \\ l_1 & l_2 & l_3 \end{Bmatrix} , \quad 6 - j \text{ symbol}, \tag{2.20}$$

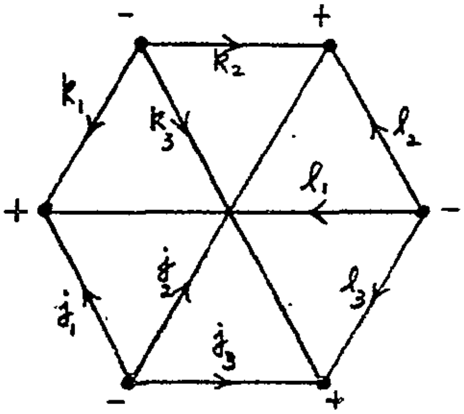

$$= \begin{Bmatrix} j_1 & j_2 & j_3 \\ l_1 & l_2 & l_3 \\ k_1 & k_2 & k_3 \end{Bmatrix}, \text{ 9-j symbol.} \tag{2.21}$$

In general, we have

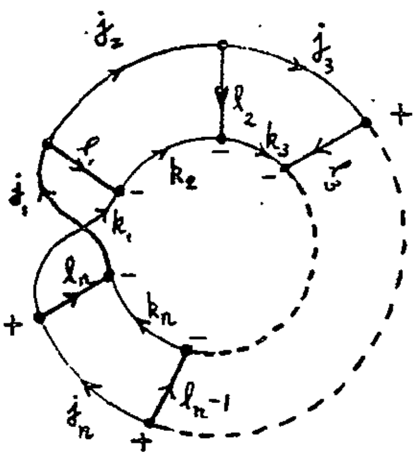

$$= \left\{ \begin{array}{cccc|c} j_1 & j_2 & \cdots\cdots & j_n & \\ l_1 & l_2 & \cdots\cdots & l_n & 1 \\ k_1 & k_2 & \cdots\cdots & k_n & \end{array} \right\} , \tag{2.22}$$

which is defined as <u>the 3n-j symbol of the first kind</u>. For n = 1, 2, 3, it equals the ordinary 3n-j symbol within a phase factor. We also have <u>the 3n-j symbol of the second kind</u>

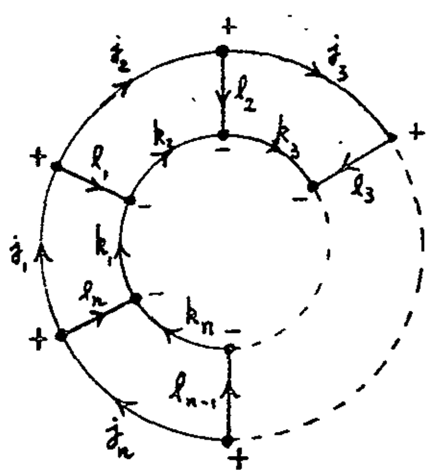

$$= \left\{ \begin{array}{cccc|c} j_1 & j_2 & \cdots\cdots & j_n & \\ l_1 & l_2 & \cdots\cdots & l_n & 2 \\ k_1 & k_2 & \cdots\cdots & k_n & \end{array} \right\} . \tag{2.23}$$

Further discussion of these 3n-j symbols may be found in the works by Jucys et al. (1962) and by El-Baz and Castel (1972). We emphasize that it is the topology of an angular-momentum diagram (i.e., how the various lines in it are connected to each other) which determines its analytical value. Therefore by keeping the topology, we can deform an angular-momentum diagram in any way without changing its analytical value.

A very complete tabulation of Clebsch-Gordan coefficients can be found in Tables of the Clebsch-Gordan Coefficients, compiled by the Institute of Atomic Energy, Academica Sinica (1965). Extensive tabulation of the 3-jm symbol and the 6-j symbol may be found in the work by Rotenberg et al. (1959). This reference also contains extensive references in the literature on 3n-j symbols.

D. The Clebsch-Gordan Coefficient

In constructing coupled angular-momentum states, where the Clebsch-Gordan coefficient (to be referred to as the C-G coefficient) occurs naturally, one finds that the graphical representation of the C-G coefficient is more expedient to use. A graphical representation (El-Baz, 1969) of the C-G coefficient is given by

$$\langle j_1 m_1 \; j_2 m_2 | j_3 m_3 \rangle \; =$$

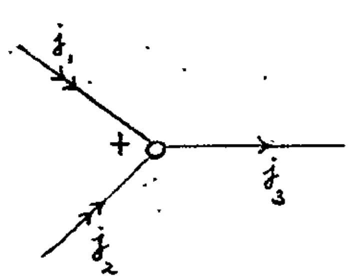

(2.24)

The notational rules to represent and to combine C-G coefficients are the same as those for 3-jm coefficients. The only difference is that we use an open circle (instead of a solid node as in the case of a 3-jm coefficient) at the vertex to represent a C-G coefficient. Although transformation rules for C-G diagrams have been given (El Baz, 1969; El-Baz and Castel, 1971, 1972), we will not present them here because we only use the graphical representation of the C-G coefficient in constructing many-particle configurations. The resulting C-G diagram will then be transformed into a 3-jm diagram by a simple procedure.

To transform a C-G diagram into a 3-jm diagram, we do the following:

(i) Add a bar, $\bar{j}$, on the angular momentum j which is unique in its variance character. The bar represents a multiplication factor $(2j+1)^{\frac{1}{2}}$.

(ii) The second (third) angular momentum k, counting from $\bar{j}$ in the direction indicated by the sign of the open circle, introduces a phase factor $(-)^{2k}$ if j is contravariant (covariant). We write a circle around the arrow of the angular-momentum line k to indicate this phase factor. When the angular-momentum line k is joined to another angular-momentum line to form a closed line, the circle representing the phase factor $(-)^{2k}$ simply changes the direction of the closed angular-momentum line k.

(iii) Fill the open circle at the vertex into a solid node and change the sign at the node.

Note the special case

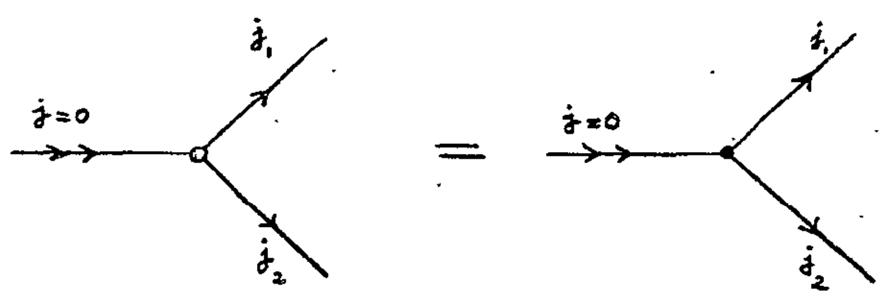

(2.25)

with the sign at the node unchanged. Similarly we have the equivalence

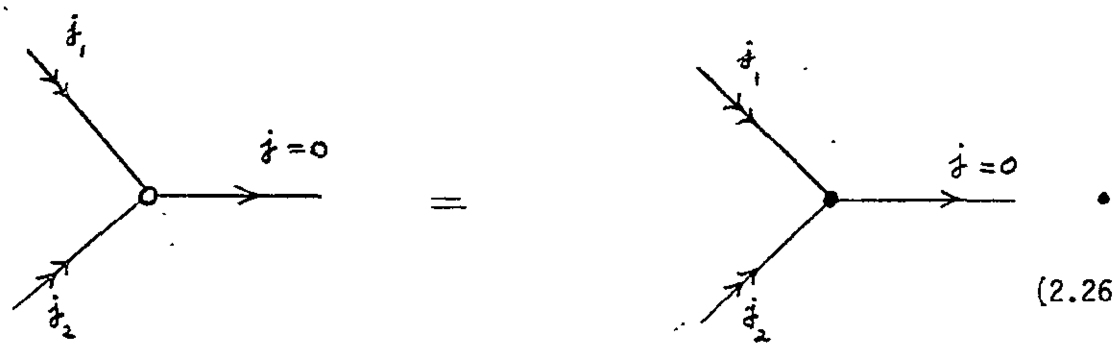

(2.26)

We will find frequent uses of these simple relations in constructing many-particle configurations.

III. ANALYTICAL EXPANSION OF ANTISYMMETRIZED MATRIX ELEMENTS

The method of evaluating matrix elements between antisymmetrized many-particle states is outlined analytically in this section. The part of the manipulation which can be performed more expediently by a graphical procedure is presented again in detail with graphical representation in the next section.

In the Dirac-Fock or Dirac-Fock-Slater description of a many-particle system, a configuration is specified by the number of equivalent particles occupying each subshell. In general, there are N_a particles in the subshell j_a, N_b particles in the subshell j_b, . . . , N_λ particles in the subshell j_λ, etc. Accordingly this configuration is denoted by

$$\left\{ j_a^{N_a} \; j_b^{N_b} \cdots \; j_\lambda^{N_\lambda} \cdots \right\} .$$

For reference purpose, we may order the subshells in a certain sequence (e.g., $1s_{1/2}$, $2s_{1/2}$, $2p_{1/2}$, etc. for atomic subshells) and refer them by successive values of the index λ.

We consider states of the many-particle system in which each subshell of equivalent particles is in a definite state with total subshell angular momenta J_a, J_b, . . . J_λ, etc. Within a subshell j_λ, if there are several states with the same total subshell angular momentum J_λ, there will be an additional quantum number α_λ which is required to specify a subshell state uniquely. This coupling scheme is indicated by

$$(j_a^{N_a})\,\alpha_a J_a \; (j_b^{N_b})\,\alpha_b J_b \; \cdots \; (j_\lambda^{N_\lambda})\,\alpha_\lambda J_\lambda \cdots$$

All the total subshell angular momenta ($J_a\ J_b\ .\ .\ .\ J_\lambda\ .\ .\ .$) are then coupled successively to form a grand total angular momentum J of the whole many-particle system. After antisymmetrization, such a state is denoted by

$$\left|\left[(j_a^{N_a})\alpha_a J_a (j_b^{N_b})\alpha_b J_b \cdots (j_\lambda^{N_\lambda})\alpha_\lambda J_\lambda \cdots\right]\alpha J M\right\rangle , \tag{3.1}$$

where α stands symbolically for the coupling scheme of total subshell angular momenta.

We will first express the matrix element between antisymmetrized many-particle states (3.1) as a sum of matrix elements between semisymmetrized many-particle states. As mentioned in Sec. I, the semisymmetrized many-particle state is defined as the many-particle state which is antisymmetric within each subshell but is not antisymmetric with respect to exchange of two particles from different subshells. Each semisymmetrized matrix element is then expanded in terms of jm-scheme matrix elements. After the evaluation of jm-scheme matrix elements, we thus obtain the expansion of the antisymmetrized matrix element in terms of reduced matrix elements, i.e., weighted radial integrals.

A. Expansion of Antisymmetrized Matrix Elements in Terms of Semisymmetrized Matrix Elements

We consider matrix elements of one-particle operators and two-particle operators in turn.

One-particle Operator

We define the one-particle operator by

$$V^{(1)} = \sum_{i=1}^{N} v_i \ . \tag{3.2}$$

From the general consideration of de-Shalit and Talmi (1963) and of Fano (1965), we can easily deduce the result

$$\langle V^{(1)}\rangle \equiv \left\langle \left[(j_a^{N_a})\alpha_a J_a \cdots (j_b^{N_b})\alpha_b J_b \cdots \right] \alpha J M \left| \sum_{i=1}^{N} v_i \right| \left[(j_a^{N_a'})\alpha_a' J_a' \cdots (j_b^{N_b'})\alpha_b' J_b' \cdots \right] \alpha' J' M' \right\rangle$$

$$= \sum_{ab} \langle V^{(1)}\rangle_{ab} \;, \tag{3.3}$$

where the summation is over all nonvanishing subshell pairs (a, b) with each pair counted once, and $\langle V^{(1)}\rangle_{ab}$ is defined as

$$\langle V^{(1)}\rangle_{ab} = (-)^{P_{ab}} \sqrt{N_a N_b'} \, \langle q(a)\alpha J M | v_N | q'(b)\alpha' J' M' \rangle \tag{3.4}$$

with

$$P_{ab} = \sum_{\lambda=a+1}^{b} N_\lambda \;. \tag{3.5}$$

Here $\langle q(a)\alpha JM|$ and $|q'(b)\alpha'J'M'\rangle$ are semisymmetrized many-particle states with definite particle distributions specified by q(a) and q'(b), respectively. Explicitly q(a) and q'(b) denote the particle distributions in which the Nth particle (i.e., the <u>active particle</u>) is in subshells a and b, respectively, while all the other particles (i.e., <u>the spectator particles</u>) assume the same distribution in both states. We emphasize that how the spectator particles are distributed among subshells is immaterial so long as they keep the same distribution in both states.

Two-particle Operator

We define the two-particle operator by

$$V^{(2)} = \sum_{i<j}^{N} v_{ij} \;. \tag{3.6}$$

Also from the general consideration of de-Shalit and Talmi (1963) and of Fano (1965), we can deduce the result

$$\begin{aligned}\langle V^{(2)}\rangle \equiv \Big\langle &\Big[(j_a^{N_a})\alpha_a J_a \cdots (j_b^{N_b})\alpha_b J_b \cdots (j_c^{N_c})\alpha_c J_c \cdots \\ &(j_d^{N_d})\alpha_d J_d \cdots\Big]\alpha J M \Big| \sum_{i<j}^{N} v_{ij} \\ &\Big|\Big[(j_a^{N_a'})\alpha_a' J_a' \cdots (j_b^{N_b'})\alpha_b' J_b' \cdots (j_c^{N_c'})\alpha_c' J_c' \cdots \\ &(j_d^{N_d'})\alpha_d' J_d' \cdots\Big]\alpha' J' M' \Big\rangle \\ = &\sum_{ab,cd} \langle V^{(2)}\rangle_{ab,cd} \;,\end{aligned} \tag{3.7}$$

where the summation is over all distinct nonvanishing pairs with $a \le b$ and $c \le d$, and $\langle V^{(2)}\rangle_{ab,cd}$ is defined as

$$\begin{aligned}\langle V^{(2)}\rangle_{ab,cd} = (-)^{P_{abcd}} &\sqrt{N_a(N_b-\delta_{ab})N_c'(N_d'-\delta_{cd})} \\ \times \Big\{ &[1+\delta_{ab}\delta_{cd}]^{-1}\langle q(ab)\alpha J M | v_{(N-1)N} | q'(cd)\alpha' J' M'\rangle \\ &-(1-\delta_{ab})(1-\delta_{cd})\langle q(ab)\alpha J M | v_{(N-1)N} | q'(dc)\alpha' J' M'\rangle\Big\}\end{aligned} \tag{3.8}$$

with

$$P_{abcd} = \sum_{\lambda=a+1}^{b}(N_\lambda - \delta_{\lambda b}) + \sum_{\lambda=c+1}^{d}(N_\lambda' - \delta_{\lambda d}) \,. \tag{3.9}$$

Here $\langle q(ab)\alpha JM|$ denotes a semisymmetrized many-particle state with the (N-1)th and Nth particles (the active particles in subshells a and b, respectively. The distribution q'(cd) and q'(dc) are defined similarly to q(ab). Again we emphasize that all of them have the same spectator-particle distribution.

B. Expansion of Semisymmetrized Matrix Elements in Terms of jm-Scheme Matrix Elements

To evaluate matrix elements between semisymmetrized many-particle states we need to single out those particles which actually participate in the interaction, i.e., the Nth particle and the (N-1)th and Nth particles in (2.4) and (2.8), respectively. This may be accomplished by fractional parentage expansions of the subshell states involving active particles. With coefficients of fractional parentage (to be referred to as c.f.p.) as expansion coefficients, the semisymmetrized many-particle state can thereby be expressed by a linear combination of parent states. Each of these parent states can then be decoupled into a product of two parts: One contains active particles, and the other contains spectator particles. These expansions and decouplings enable us to express a semisymmetrized matrix element in terms of jm-scheme matrix elements. We consider the cases for one-particle operators and for two-particle operators in turn:

<u>One-particle operator</u>

To evaluate the semisymmetrized matrix element in (3.4) we first decouple the semisymmetrized many-particle states as

$$\langle q(a)\alpha JM| = \sum_{p} C_a(p;\alpha JM)\langle p; q(a)|\langle a| \qquad (3.10)$$

and

$$|q'(b)\alpha'J'M'\rangle = \sum_{p'} C_b(p';\alpha'J'M')|p';q'(b)\rangle|b\rangle . \tag{3.11}$$

Here $\langle p;q(a)|$ and $|p';q'(b)\rangle$ denote symbolically the uncoupled subshell states of the spectator particles, i.e., the first (N-1) particles; $\langle a|$ and $|b\rangle$, or explicitly $\langle j_a m_a|$ and $|j_b m_b\rangle$, are the orbitals of the active particle, i.e., the Nth particle. The expansion coefficient $C_a(p;\alpha JM)$ or $C_b(p';\alpha'J'M')$ stands symbolically for the product of a c.f.p. and all the 3-jm coefficients needed in the uncoupling, and the summation index p or p' for the summation over the c.f.p. and magnetic quantum numbers. Explicit examples will be given in Sec. IV.B when we consider the graphical procedure. By using (3.10) and (3.11), we can write the semisymmetrized matrix element in (3.4) as

$$\langle q(a)\alpha JM|v_N|q'(b)\alpha'J'M'\rangle$$

$$= \sum_{pp'} C_a(p;\alpha JM)C_b(p';\alpha'J'M')\langle p;q(a)|p';q'(b)\rangle\langle a|v_N|b\rangle. \tag{3.12}$$

Here the matrix element $\langle p;q(a)|p';q'(b)\rangle$ represents a product of overlap integrals and is independent of the interaction. The matrix element $\langle a|v_N|b\rangle$, called the jm-scheme matrix element, depends on the interaction and will be evaluated in the next subsection. Interested readers may refer to (4.15) for the graphical representation of (3.12).

Two-particle operator

We decouple the semisymmetrized many particle states in (3.8) and obtain

$$\langle q(ab)\alpha JM| = \sum_{p} C_{ab}(p;\alpha JM)\langle p;q(ab)|\langle ab| \tag{3.13}$$

and

$$|q'(cd)\alpha' J' M'\rangle = \sum_{p'} C_{cd}(p';\alpha' J' M')|p';q'(cd)\rangle|cd\rangle. \tag{3.14}$$

Here $\langle p;q(ab)|$ and $\langle p';q'(cd)|$ stand symbolically for the uncoupled subshell states of the spectator particles, i.e., the first (N-2) particles; $\langle ab|$ and $|cd\rangle$, or explicitly $\langle j_a m_a\ j_b m_b|$ and $|j_c m_c\ j_d m_d\rangle$, for the active particles, i.e., the (N-1)th and Nth particles; $C_{ab}(p;\alpha JM)$ and $C_{cd}(p';\alpha' J' M')$ for the expansion coefficients which are products of c.f.p. and 3-jm coefficients; p and p' for all the summation indices involved. Explicit examples will be given in Sec. IV.B. Note that here a and b (also c and d) may represent either equivalent or nonequivalent orbitals.

By means of the expansions (3.13) and (3.14) we obtain the first semi-symmetrized matrix element (the direct term) in (3.8) as

$$\begin{aligned}\langle q(ab)\alpha JM|&V_{N-1,N}|q'(cd)\alpha' J' M'\rangle \\ &= \sum_{pp'} C_{ab}(p;\alpha JM)\, C_{cd}(p';\alpha' J' M')\langle p;q(ab)|p';q'(cd)\rangle \\ &\quad \times \langle ab|V_{N-1,N}|cd\rangle. \end{aligned} \tag{3.15}$$

Here the matrix element $\langle p;q(ab)|p';q'(cd)\rangle$ represents a product of overlap integrals, and $\langle ab|v_{N-1,N}|cd\rangle$ is a jm-scheme matrix element. The second semisymmetrized matrix element (the exchange term) in (3.8) can be expanded similarly as (3.15) in terms of jm-scheme matrix elements. Interested readers may refer to (4.16) for the graphical representation of (3.15).

C. jm-Scheme Matrix Elements

In the last subsection, we have shown how a semisymmetrized matrix element can be expended as a sum of products of two parts: One is the interaction-independent part involving the coupling coefficients, and the other is the interaction-dependent part represented by a jm-scheme matrix element. The jm-scheme matrix elements for the cases of one-particle operators and two-particle operators are given by $\langle a|v_N|b\rangle$ and $\langle ab|v_{N-1,N}|cd\rangle$, respectively. For specific operators, these matrix elements can be evaluated analytically in terms of radial integrals. The results for commonly used operators and potentials are presented in Appendix B along with their graphical forms.

In general, any operator can be written as a sum of products of irreducible tensor operators. Hence in this subsection for a general purpose, we consider v_N and $v_{N-1,N}$ to be irreducible tensor operators. The results are given in terms of reduced matrix elements as follows.

One-particle operator

Assume the one-particle operator v_N to be an irreducible tensor operator of degree j,

$$v_N = T_{jm}(N) . \tag{3.16}$$

By applying the Wigner-Eckart theorem (Wigner, 1927; Eckart, 1930) we obtain the jm-scheme matrix element in (3.12) as

$$\langle a|v_N|b\rangle \equiv \langle j_a m_a | T_{jm} | j_b m_b \rangle$$
$$= \begin{pmatrix} j_a & m & m_b \\ m_a & j & j_b \end{pmatrix} \langle j_a || T^{(j)} || j_b \rangle . \tag{3.17}$$

Here we denote the angular momentum coupling by a covariant 3-jm coefficient, and $<j_a||T^{(j)}||j_b>$ is the reduced matrix element which is usually expressible as a sum of weighted radial integrals for a specific case. It is of interest to note that the bra (covariant) state $<j_a m_a|$ corresponds to the covariant component in the 3-jm coefficient, and the contravariant operator T_{jm} and the ket (contravariant) state $|j_b m_b>$ correspond to the two contravariant components. No extra phase or weight factor, besides the reduced matrix element, is carried by (3.17), and the rotational properties of the matrix element is clearly indicated by the 3-jm coefficient.

To emphasize the fact that the jm-scheme matrix element is separated into a geometric part and a dynamical part, we rewrite (3.17) as

$$\langle a|v_N|b\rangle = G_j(a;b)\, X_j(a;b). \tag{3.18}$$

The geometric factor $G_j(a;b)$, which corresponds to a coupling diagram in the graphical representation and will be called <u>the interaction graph</u>, is defined in this simple case as

$$G_j(a;b) = \begin{pmatrix} j_a & m & m_b \\ m_a & j & j_b \end{pmatrix}. \tag{3.19}$$

<u>The interaction strength</u> $X_j(a;b)$ is defined accordingly as

$$X_j(a;b) = \langle j_a || T^{(j)} || j_b \rangle . \tag{3.20}$$

Two-particle operator

For the case of a two-particle operator, we consider an irreducible tensor of degree j which is the tensorial product of two irreducible tensor operators acting on two different particles, i.e.,

$$\mathcal{V}_{N-1,N} = T_{jm}(N-1,N) \equiv \sum_{m_1 m_2} \langle j_1 m_1 j_2 m_2 | j m \rangle T_{j_1 m_1}(N-1)\, T_{j_2 m_2}(N) \tag{3.21}$$

As before, by applying the Wigner-Eckart theorem we can obtain the jm-scheme matrix element in (3.15) as

$$\begin{aligned}\langle ab | \mathcal{V}_{N-1,N} | cd \rangle &\equiv \langle j_a m_a j_b m_b | T_{jm}(N-1,N) | j_c m_c j_d m_d \rangle \\ &= G_j(ab;cd)\, X_{j_1 j_2}(ab;cd).\end{aligned} \tag{3.22}$$

Here the geometric factor $G_j(ab;cd)$ is given by

$$G_j(ab;cd) = (2j+1)^{1/2} \sum_{m_1 m_2} \begin{pmatrix} j_a & j_1 & m_c \\ m_a & m_1 & j_c \end{pmatrix} \begin{pmatrix} m_1 & m & j_2 \\ j_1 & j & m_2 \end{pmatrix} \begin{pmatrix} j_b & m_2 & m_d \\ m_b & j_2 & j_d \end{pmatrix}, \tag{3.23}$$

and the interaction strength by

$$X_{j_1 j_2}(ab;cd) = \langle j_a \| T^{(j_1)} \| j_c \rangle \langle j_b \| T^{(j_2)} \| j_d \rangle . \tag{3.24}$$

D. Expansion of Antisymmetrized Matrix Elements in Terms of Reduced Matrix Elements

In Sec. III.A we expanded the matrix element between antisymmetrized many-particle states as a sum of semisymmetrized matrix elements. In Sec.

III.B we obtained the semisymmetrized matrix element in terms of jm-scheme matrix elements, which were later evaluated in Sec. III.C. Here we summarize the results.

One-particle operator

For $V^{(1)} = \sum_{i=1}^{N} T_{jm}(i)$, the antisymmetrized matrix element (3.3) has been evaluated as

$$\langle \alpha J M | V^{(1)} | \alpha' J' M' \rangle = \sum_{ab} (-)^{P_{ab}} (N_a N_b')^{1/2} \times \mathcal{D}_{jm}(a;b) X_j(a;b), \tag{3.25}$$

where the coupling coefficient $D_{jm}(a;b)$ is given by

$$\mathcal{D}_{jm}(a;b) = \sum_{pp'} C_a(p;\alpha J M) C_b(p';\alpha' J' M') \langle p; q(a) | p'; q'(b) \rangle \times G_j(a;b). \tag{3.26}$$

Two-particle operator

For $V^{(2)} = \sum_{i<j}^{N} T_{jm}(ij)$ with $T_{jm}(ij)$ defined in (3.21), we can summarize the results for the antisymmetrized matrix element (3.7) as

$$\langle \alpha J M | V^{(2)} | \alpha' J' M' \rangle = \sum_{ab,cd} (-)^{P_{abcd}} [N_a(N_b - \delta_{ab}) N_c'(N_d' - \delta_{cd})]^{1/2}$$
$$\times \Big\{ [1 + \delta_{ab}\delta_{cd}]^{-1} \mathcal{D}_{jm}(ab;cd) X_{j_1 j_2}(ab;cd)$$
$$- (1-\delta_{ab})(1-\delta_{cd}) \mathcal{D}_{jm}(ab;dc) X_{j_1 j_2}(ab;dc) \Big\}. \tag{3.27}$$

Here the coupling coefficient $D_{jm}(ab;cd)$ is defined as

$$D_{jm}(ab;cd) = \sum_{pp'} C_{ab}(p;\alpha JM)\, C_{cd}(p';\alpha' J' M') \langle p;q(ab) | p';q'(cd) \rangle$$

$$\times G_j(ab;cd) \,, \tag{3.28}$$

with $D_{jm}(ab;dc)$ similarly defined. The interaction strength $X_{j_1 j_2}(ab;cd)$ has been given in (3.24), and $X_{j_1 j_2}(ab;dc)$ is given by a similar expression with c and d interchanged.

IV. GRAPHICAL EVALUATION OF SEMISYMMETRIZED MATRIX ELEMENTS

Evaluation of the coupling coefficients $D_{jm}(a;b)$ and $D_{jm}(ab;cd)$, given in (3.26) and (3.28), respectively, is a formidable task. Although for many cases they may be evaluated numerically (Grant, 1973; 1976) by using a digital computer, these coupling coefficients in general have to be obtained analytically for each particular case, especially for the analytical study of a matrix element. In this section we will show how to obtain an analytical expression of an antisymmetrized many-particle matrix element from easily constructed diagrams.

In Sec. IV.A the graphical procedure of constructing semisymmetrized many-particle states is illustrated by an example. Section IV.B describes how to decouple graphically particles from an antisymmetrized subshell state. The bra and ket diagram blocks are also defined there. In Sec. IV.C the jm-scheme matrix element is considered. Its graphical representation is defined as the interaction block. Specific diagrams are given for the cases considered analytically in Sec. III.C. Other interaction diagrams for commonly used operators and potentials are presented in Appendix B. In Sec. IV.D the spectator block is defined. Evaluation of the joined diagram, called the recoupling diagram, is described in Sec. IV.E.

A. Construction of Semisymmetrized Many-Particle States

The construction of diagrams for semisymmetrized many-particle states ca[n] easily be carried out in the C-G representation. The procedure is best demonstrated by working with an example.

Consider a configuration having open shells a, b, c, d, and closed shells λ, etc. A particular coupling scheme of the open shells is represented by

$$|[(J_aJ_b)J_{ab}(J_cJ_d)J_{cd}]JM\rangle$$

where J_a, J_b, J_c, J_d are the total angular momenta of respective subshells, and the parentheses specify the sequence of the couplings. These couplings can be given analytically by

$$|[(J_aJ_b)J_{ab}(J_cJ_d)J_{cd}]JM\rangle$$

$$= \sum_{M_{ab}M_{cd}} |(J_aJ_b)J_{ab}M_{ab}\rangle|(J_cJ_d)J_{cd}M_{cd}\rangle\langle J_{ab}M_{ab}J_{cd}M_{cd}|JM\rangle$$

$$= \sum_{M_{ab}M_{cd}} \sum_{M_aM_b} \sum_{M_cM_d} |J_aM_a\rangle|J_bM_b\rangle|J_cM_c\rangle|J_dM_d\rangle$$

$$\times \langle J_aM_aJ_bM_b|J_{ab}M_{ab}\rangle\langle J_cM_cJ_dM_d|J_{cd}M_{cd}\rangle\langle J_{ab}M_{ab}J_{cd}M_{cd}|JM\rangle \ , \quad (4.1)$$

which corresponds to the graphical representation

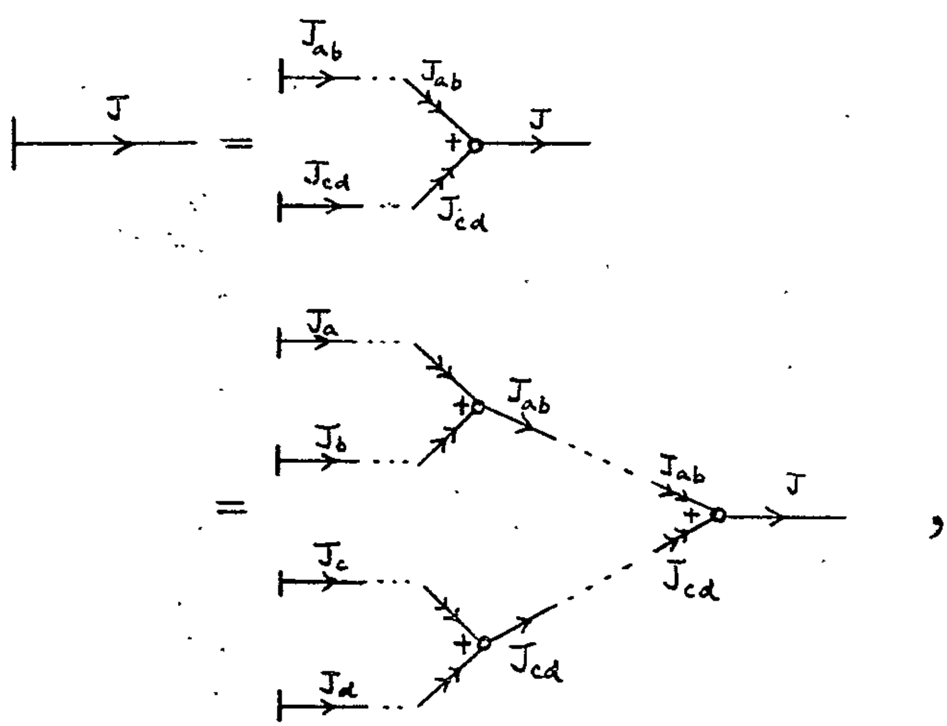

(4.2a)

or simply,

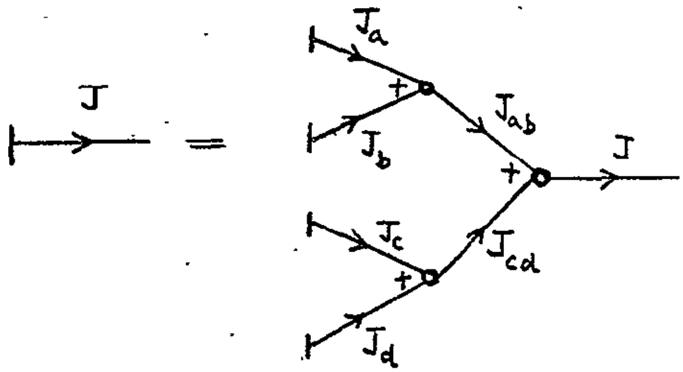

(4.2b)

All the closed shells are represented symbolically by

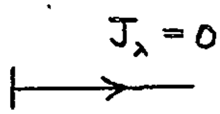

Hence the semisymmetrized many-particle state has the graphical representation

$$|J_\lambda [(J_a J_b) J_{ab} (J_c J_d) J_{cd}] JM\rangle$$

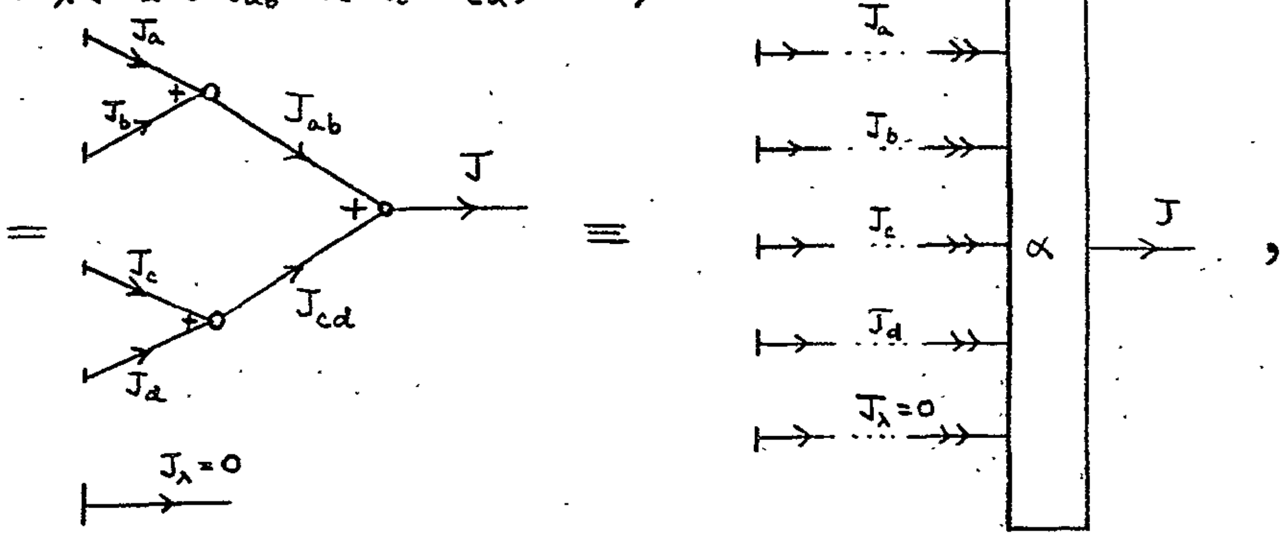

(4.3)

where α denotes symbolically the coupling scheme of the open shells.

From the above example we can generalize the following graphical procedure for constructing the semisymmetrized bra and ket states:

(i) Represent the grand total angular momentum by a line.

(ii) Draw two branches from the grand total angular momentum and a small circle at the vertex. The two angular-momentum lines added represent the two angular-momenta which are coupled to form the grand total angular momentum. Write a sign, + or -, at the vertex to indicate the order of coupling.

(iii) Repeat step (ii), starting from the new angular-momentum lines, until all subshells containing active particles are decoupled.

(iv) Add angular-momentum lines for closed shells.

(v) Mark appropriate arrows on the angular-momentum lines.

It is more convenient to construct bra (covariant) states from left to right and ket (contravariant) states from right to left. The so-constructed configuration diagrams are to be transformed into diagrams in the 3-jm representation by using the procedure given in Sec. II.D.

B. Decoupling of Active Particles; Bra Block and Ket Block

As stated in Sec. III.B, we can single out active particles from a subshell by a fractional parentage expansion. We consider two cases in turn.

One-particle coefficient of fractional parentage

To single out one particle from a subshell we use a one-particle fractional parentage expansion, i.e.,

$$\left|(j^n)\alpha JM\right\rangle = \sum_{\alpha_1 J_1} \left[(j^{n-1})\alpha_1 J_1 j \middle| \alpha J \right] \times \left|(j^{n-1})\alpha_1 J_1 j JM\right\rangle$$

$$= \sum_{\substack{\alpha_1 J_1 \\ M_1 m}} \left[(j^{n-1})\alpha_1 J_1 j \middle| \alpha J \right] \langle J_1 M_1 jm | JM \rangle \times \left|(j^{n-1})\alpha_1 J_1 M_1\right\rangle |jm\rangle . \tag{4.4}$$

Here to indicate more clearly the coupling, we use the abbreviated notation

$$\left[(j^{n-1})\alpha_1 J_1 j \middle| \alpha J \right] \equiv \left[j^{n-1}(\alpha_1 J_1) jJ \middle|\right\} j^n \alpha J \right] \tag{4.5}$$

for the c.f.p. defined by Racah (1943).

The last expression in (4.4) gives the explicit form of (3.11) in the particular case of one subshell. This decoupling can be represented by the diagram

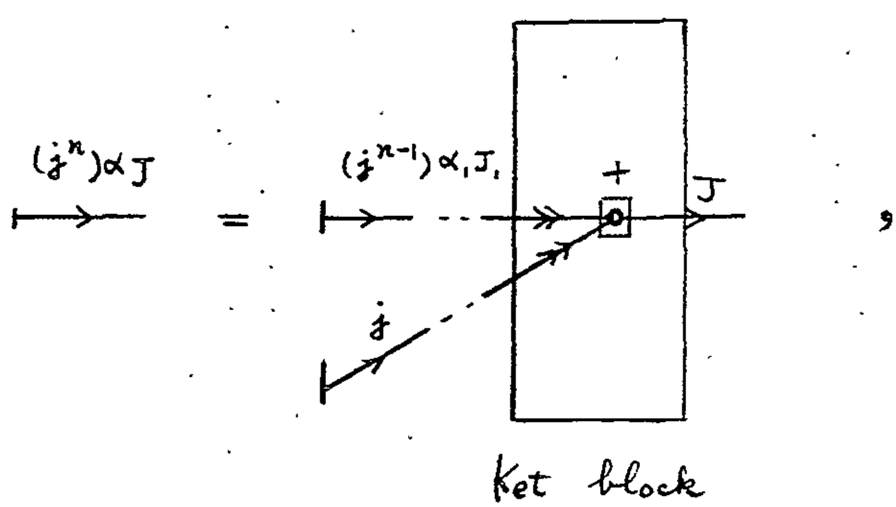

(4.6)

where the c.f.p. $[(j^{n-1})\alpha_1 J_1 j|\alpha J]$ and the summation over it are implied by the square $\square$ at the vertex $(J_1\ j\ J)$. The ket block is defined as the portion of the diagram indicated in (4.6); a bra block is similarly defined in the case of a covariant state.

Two-particle coefficient of fractional parentage

To single out two particles from a subshell we use a two-particle fractional parentage expansion, i.e.,

$$
\begin{aligned}
|(j^n)\alpha J M\rangle &= \sum_{\alpha_2 J_2 J'} [(j^{n-2})\alpha_2 J_2 (j^2) J' | \alpha J] \\
&\qquad |(j^{n-2})\alpha_2 J_2 (j^2) J' J M\rangle \\
&= \sum_{\substack{\alpha_2 J_2 J' \\ M_2 M' \\ m\ m'}} [(j^{n-2})\alpha_2 J_2 (j^2) J' | \alpha J] \\
&\qquad \times \langle j m\ j m' | J' M'\rangle \langle J_2 M_2 J' M' | J M\rangle \\
&\qquad \times |(j^{n-2})\alpha_2 J_2 M_2\rangle |j m\rangle |j m'\rangle ,
\end{aligned} \tag{4.7}
$$

where we have used the abbreviated notation

$$
[(j^{n-2})\alpha_2 J_2 (j^2) J' | \alpha J] \equiv [j^{n-2}(\alpha_2 J_2) j^2 (J') J |\} j^n \alpha J] \tag{4.8}
$$

to represent the two-particle c.f.p. The last expression of (4.7) gives the explicit example for separating two equivalent electrons from a subshell, which was given symbolically in (3.14).

The graphical representation of (4.7) is given by

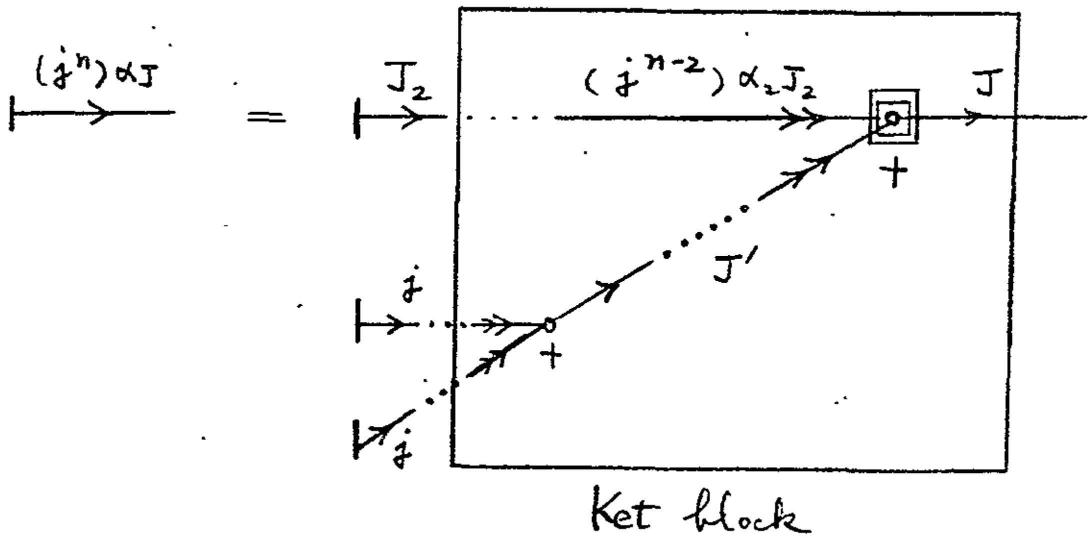

(4.9)

where the two-particle c.f.p. $[(j^{n-2})\alpha_2 J_2 (j^2) J' | \alpha J]$ and the summation over it are denoted by the double squares at the vertex $(J_2 J' J)$. The ket block is defined as indicated in (4.9); a bra block is defined in the case of a covariant state.

Tables of c.f.p. may be found in the works of Edmonds and Flowers (1952) de Shalit and Talmi (1963), and Sivcev et al. (1974).

C. Interaction Block

An interaction block refers to the diagram block representing $\langle a|v_N|b\rangle$ i the case of a one-particle operator and $\langle ab|v_{N-1,N}|cd\rangle$ in the case of a two-particle operator. These jm-scheme matrix elements have been given analytically for general cases in Sec. III.C. Besides a dynamical multiplication factor, the interaction strength, the jm-scheme matrix elements depend only on the rotational properties of the interaction and states involved. We present here the interaction blocks for the general operators worked out in Sec. III.C. Specific examples will be given in Appendix B. Again we consider two cases in turn:

One-particle operator

An elementary interaction is represented by an irreducible tensor operator T_{jm} of degree j. Its jm-scheme matrix element was given in (3.18) and has the graphical representation

$$\langle a | v_N | b \rangle =$$

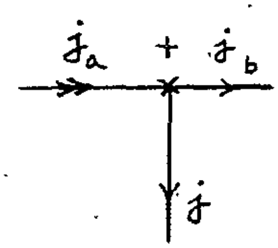

,

(4.10)

where the coupling coefficient $G_j(a;b)$ is represented by the coupling diagram and the interaction strength $X_j(a;b)$ is denoted by the cross "X" at the vertex $(j_a\ j\ j_b)$. More complicated interactions can be expressed as a linear combination of this elementary interaction.

Two-particle operator

We assume the elementary two-particle interaction to be the irreducible tensor operator $T_{jm}(N-1, N)$ defined in (3.21). Hence from (3.22) we obtain the graphical representation

$$\langle ab | v_{N-1,N} | cd \rangle =$$

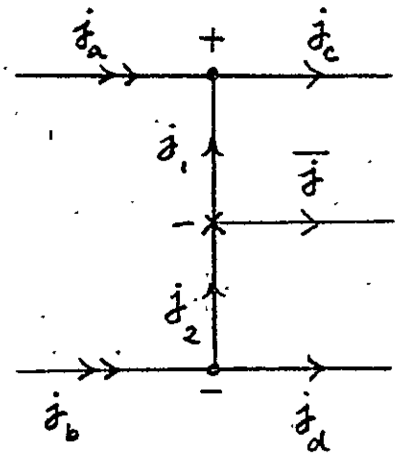

(4.11)

Here the cross "X" at the vertex $(j_1\ j\ j_2)$ denotes the interaction strength $X_{j_1 j_2}(ab;cd)$; the bar on the angular momentum $\bar{j}$ represents the multiplication factor $(2j+1)^{\frac{1}{2}}$.

D. Spectator Block

A spectator block refers to the diagram block representing the scalar product of subshell states or groups of subshell states which do not participate in the interaction considered in the semisymmetrized matrix element. It examples were given as $\langle p;q(a)|p';q'(b)\rangle$ in (3.12) and $\langle p;q(ab)|p';q'(cd)\rangle$ in (3.15). As mentioned in Sec. III.A, the spectator particles have the same distribution among subshells in both the bra and ket states. This fact implies that the scalar product of the composite states can be written as a product of overlap integrals for all subshells. Graphically, we represent spectator blocks as follows.

(i) $<p;q(a)|p';q'(b)>$

$=$

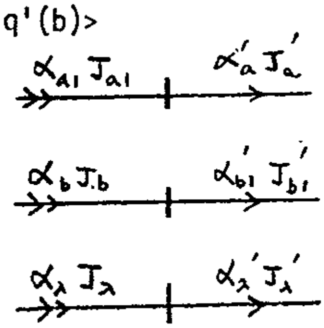

,

(4.12)

where $\alpha_{a1}J_{a1}$ and $\alpha'_{b1}J'_{b1}$ are parent states of subshells a and b after the active particle being decoupled out; $\alpha_\lambda J_\lambda$ and $\alpha'_\lambda J'_\lambda$ denote symbolically all the other subshell states or groups of subshell states. From (2.16) we know that (4.12) represent a product of Kronecker deltas for the states involved, provided we use the same orthonormal set of particle orbitals in both the bra and ket states.

(ii) $<p;q(ab)|p';q'(cd)>$

$=$

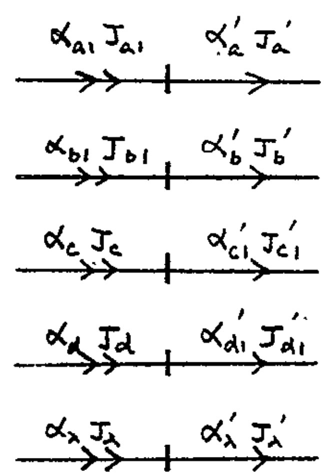

,

(4.13)

where the notations are defined similarly as in the case (i). Another example is given by

$$\langle p; q\,(a^2) \,|\, p'; q'\,(cd) \rangle$$

$$=$$

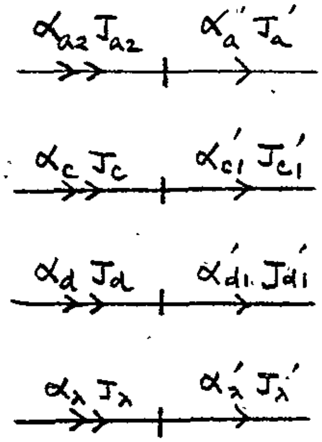

, (4.14)

where $\alpha_{a2}J_{a2}$ is the state of subshell $\underline{a}$ after two active particles being decoupled out by a two-particle fractional parentage expansion.

The graphical rule implied by (4.12), (4.13), and (4.14) is that we simply join together the corresponding (covariant-contravariant) angular-momentum lines in the bra and ket blocks. Note however that this simple graphical rule does not apply when particle orbitals in the bra state are not orthonormal to those in the ket state. In such cases we need an extra factor which is the product of all the overlap integrals of the spectator particles of the bra and ket states.

E. Evaluation of Recoupling Diagrams

In Sec. IV.A we demonstrated how to construct diagrams for semisymmetrized many-particle states, and a simple graphical procedure was given. In Sec. IV.B we showed how to separate graphically active particles from a subshell. There, the part of the configuration diagram involving expansion coefficients and angular-momentum couplings constituted the bra block or the ket block in the case of a covariant state or contravariant state, respectively. In Sec. IV.C and IV.D, we defined the interaction block and the spectator block; their typical diagrams were given. Here we summarize the results by the symbolic diagrams:

(i) $\langle q(a)\alpha JM|\, v_N\, |q'(b)\alpha' J'M'\rangle$

=

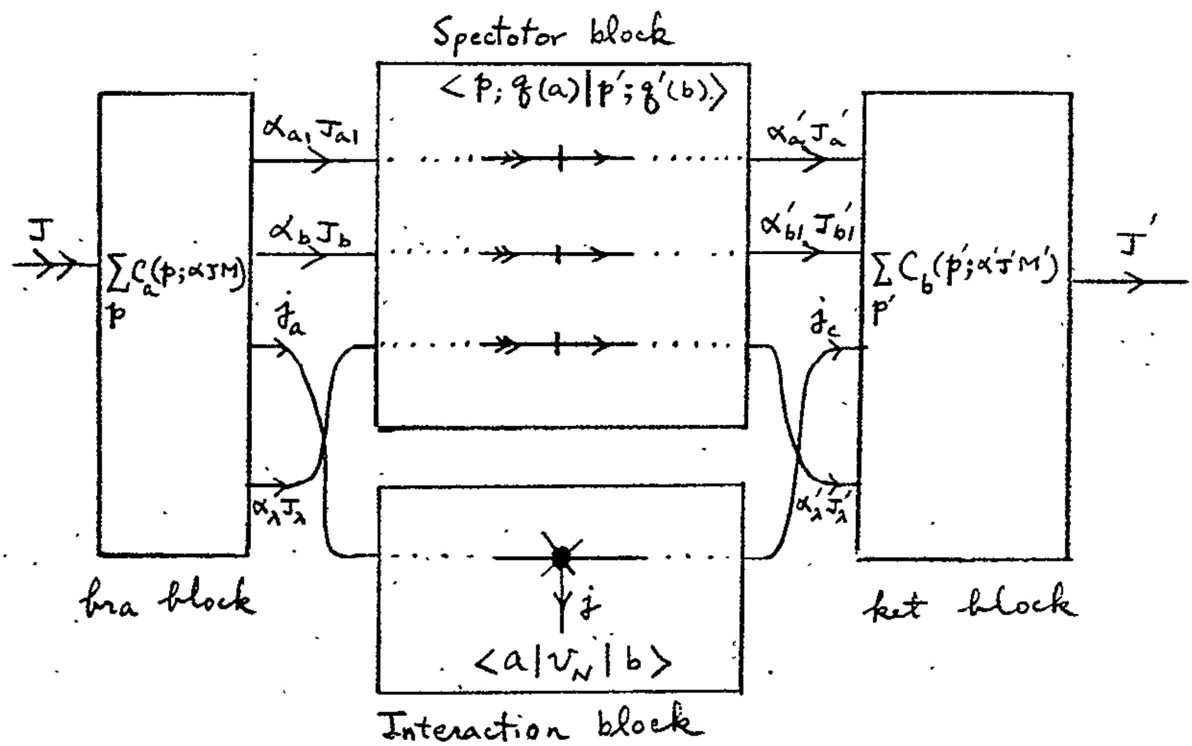

.

(4.15)

(ii) $\langle q(ab)\alpha JM|v_{N-1,N}|q'(cd)\alpha'J'M'\rangle =$

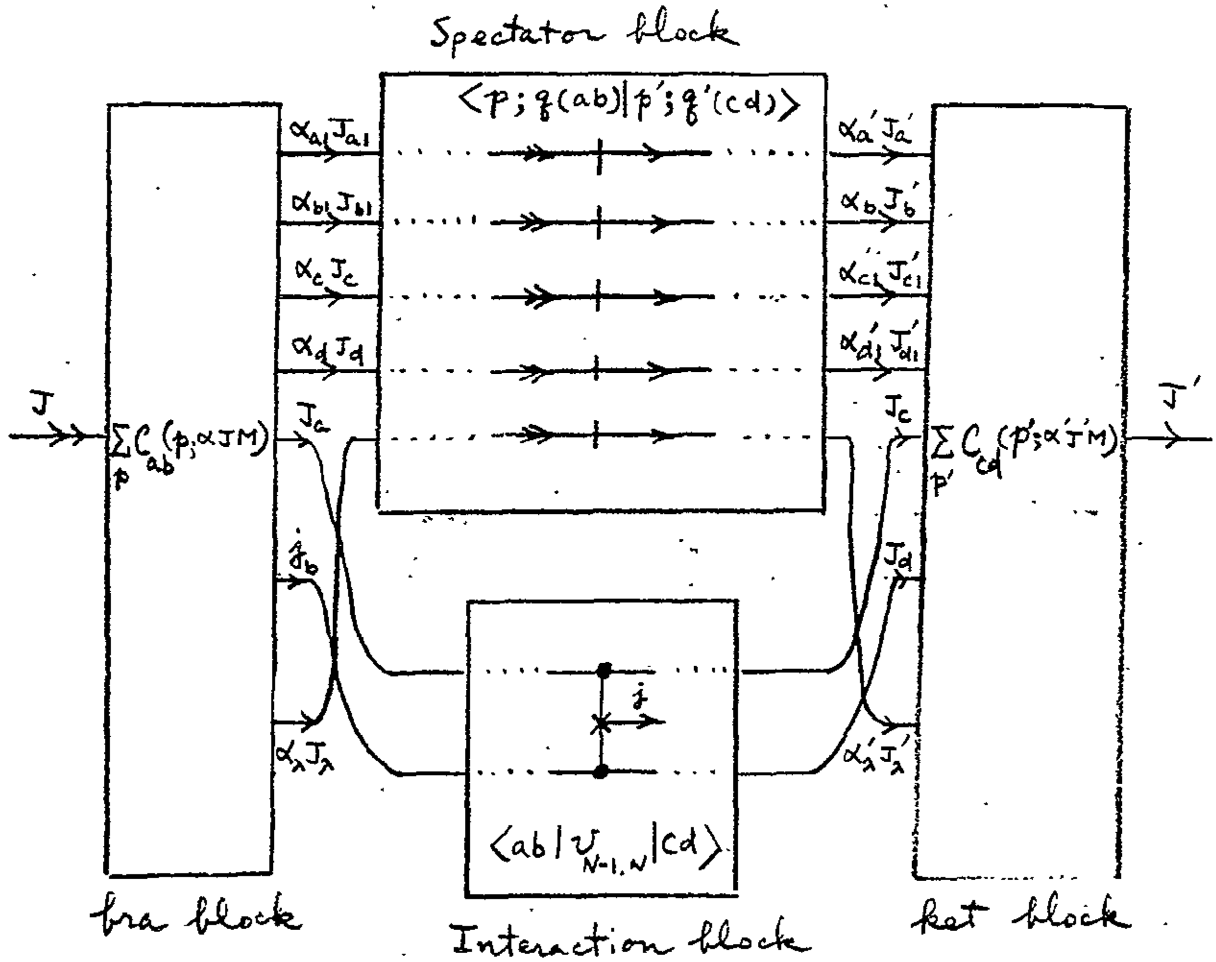

(4.16)

After extracting the interaction strength, c.f.p., and summations over them i (4.15) or (4.16), we are in general left with a pure angular-momentum-coupling diagram, i.e.,

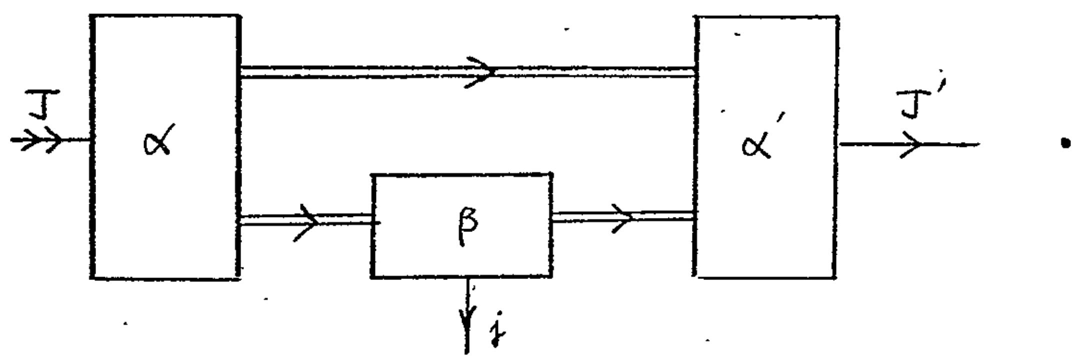

(4.17)

Here the double-lines stand symbolically for all angular-momentum lines connecting two diagram blocks. By using the transformation rule (2.14), we obtain

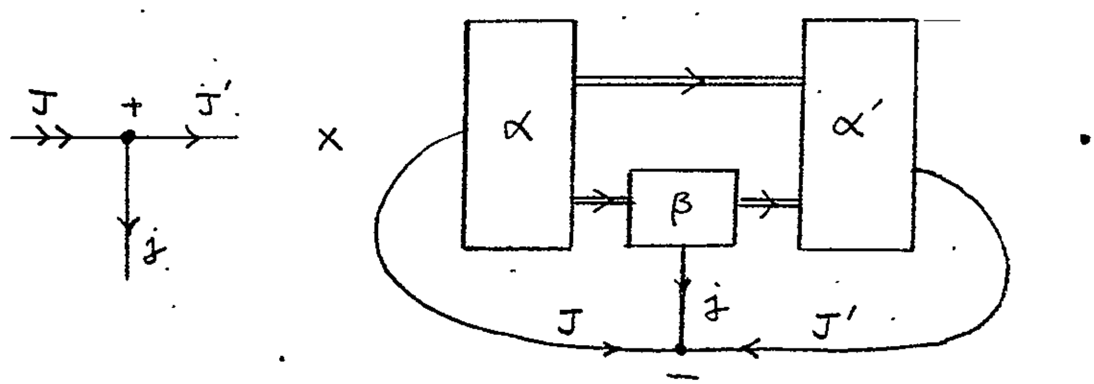

(4.18)

The first factor in (4.18) represents a 3-jm coefficient, which is to be expected by applying directly the Wigner-Eckart theorem to the semisymmetrizec matrix element. The second factor in (4.18) is a <u>recoupling diagram</u> representing analytically a recoupling coefficient. By using transformation rules given in Sec. II.B, we can express the recoupling diagram in terms of products of 3n-j diagrams whose analytical values have been tabulated extensively (Rotenberg et al., 1959; Jucys et al., 1962).

The most expedient way to factor graphically a recoupling diagram into 3n-j diagrams depends, of course, on the particular diagram in question. A simple rule is to look first for diagram blocks separable on one angular-momentum line and then on two and three angular-momentum lines.

V. SUMMARIZED PROCEDURE FOR EVALUATING ANTISYMMETRIZED MATRIX ELEMENTS

In this section the results of Sec. III and IV will be summarized in the form of a step-by-step procedure by which matrix elements of operators or potentials between antisymmetrized many-particle states can be evaluated. The prescription is given as follows.

(i) Follow (3.3) and (3.4) for one-particle operators, or (3.7) and (3.8) for two-particle operators to express the antisymmetrized matrix element as a sum of semisymmetrized matrix elements.

(ii) For each semisymmetrized matrix element, construct graphically semisymmetrized many-particle states:

(a) Begin with the grand total angular momentum and the two angular momenta coupled to it. Here we use the bra state to illustrate the procedure:

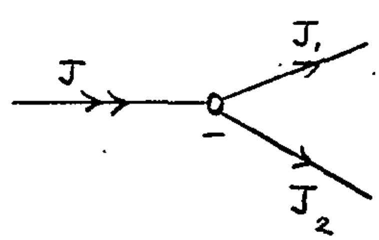

(5.1)

(b) Repeat step (a) starting from J_1 and J_2 until all active subshells are decoupled. Closed shells are then added separately. The resultant diagram is given schematically as

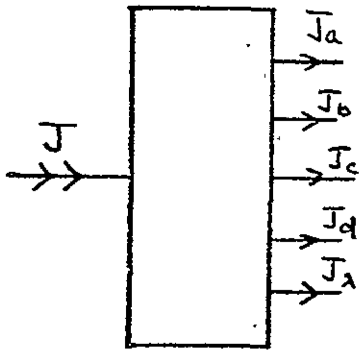

(5.2)

Note that in constructing semisymmetrized many-particle states those subshells which neither involve coupling with other subshells nor contain active particles may be ignored.

The ket state is constructed similarly.

(iii) Decouple active particles from respective subshells by making use of the fractional parentage expansions (4.6) or (4.9), e.g.,

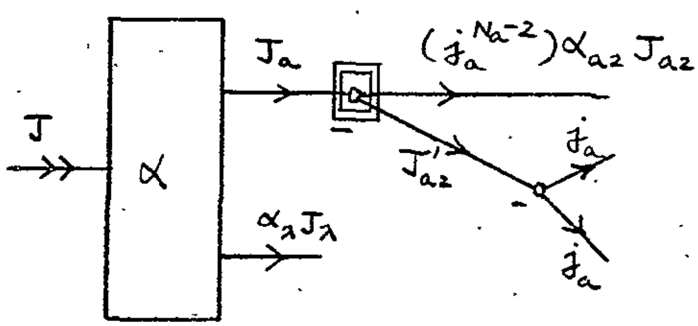

(5.3)

(iv) Repeat steps (ii) and (iii) for the ket state.

(v) Insert the interaction block between lines representing active particles, and connect the corresponding spectator-particle lines in the bra and ket states. Here the interaction strength in the interaction block can be obtained analytically. A summary of the interaction strengths for various commonly used operators and potentials is given in Appendix B.

(vi) Transform the C-G representation of the bra and ket states into the 3-jm representation by using the transformation procedure presented in Sec. II.D.

(vii) Transcribe analytical expressions from symbols representing the interaction strength, the c.f.p.'s and the summations association with them. The rest of the diagram represents a standard recoupling diagram which may be reduced to an analytical expression. The transformation rules to reduce an arbitrary recoupling diagram to tabulated 3n-j coefficients is given in Sec. II.B.

(viii) Repeat steps (ii)-(vii) for other non-vanishing subshell pairs, as indicated in step (i). The final expression of the antisymmetrized matrix element is thus obtained by summarizing all the analytical expressions resulted in step (vii).

VI. EXAMPLE

We illustrate the graphical procedure by an example:

Consider the C-AB;D Auger transition (Auger, 1925; Bambynek et al., 1972 in a rare gas ion, where C denotes the initial vacancy in subshell C, and the final state is characterized by one vacancy in each of subshells A and B plus an outgoing electron D. This is one of the de-excitation processes of an atom with an inner-shell vacancy, in which the transition energy from filling the inner-shell vacancy by an outer-shell electron is carried off by the ejection of another outer-shell electron. The transition probability amplitude is given in the Dirac-Fock formulation by (Huang, 1978a)

$$T_{if}(C-AB;D) = \Big\langle \big[J_\lambda (j_a^{n_a}) \alpha_a J_a (j_b^{n_b}) \alpha_b J_b (j_c^{n_c}) \alpha_c J_c \big] \alpha J M \Big| \times \sum_{i<j}^{N} V_{ij} \Big| \big[J_\lambda (j_a^{n_a'}) \alpha_a' J_a' (j_b^{n_b'}) \alpha_b' J_b' (j_c^{n_c'}) \alpha_c' J_c' j_d \big] \alpha' J' M' \Big\rangle \tag{6.1}$$

with

$$V_{ij} = \frac{1}{r_{ij}} - (\vec{\alpha}_i \cdot \vec{\alpha}_j) \frac{e^{i\omega r_{ij}}}{r_{ij}} + (\vec{\alpha}_i \cdot \vec{\nabla}_i)(\vec{\alpha}_j \cdot \vec{\nabla}_j) \frac{e^{i\omega r_{ij}} - 1}{\omega^2 r_{ij}} , \tag{6.2}$$

where the bra state is the initial state and the ket state is the final state with j_d the angular momentum of the continuum electron. Here all the other closed shells are denoted symbolically by J_λ. To focus on the essential feature, we assume that the same orthonormal set of single-particle orbitals is used for both the final and initial states. By applying the step-by-step procedure in Sec. V, we evaluate the antisymmetrized matrix element (6.1) as follows.

Step (i): There is only one nonvanishing subshell pair, i.e.,

$$T_{if}(C^{-}AB;D) = \left\langle \sum_{i<j}^{N} V_{ij} \right\rangle_{ab,cd} \tag{6.3}$$

with

$$\begin{aligned}
N_a &= 2j_a + 1 \quad ; \quad & N_a' &= 2j_a \\
N_b &= 2j_b + 1 & N_b' &= 2j_b \\
N_c &= 2j_c & N_c' &= 2j_c + 1 \\
N_d &= 0 & N_d' &= 1 \quad ,
\end{aligned} \tag{6.4}$$

and

$$\begin{aligned}
P_{abcd} &= \sum_{\lambda=a+1}^{b} (N_\lambda - \delta_{\lambda b}) + \sum_{\lambda=c+1}^{d} (N_\lambda' - \delta_{\lambda d}) \\
&= (\text{even number}) - 1 + (\text{even number}) - 2 \\
&= \text{odd number} .
\end{aligned} \tag{6.5}$$

Hence from (3.8) we can rewrite (6.3) as

$$T_{if}(C-AB;D) = -\left[(2j_a+1)(2j_b+1)(2j_c+1)\right]^{1/2}$$

$$\times\left\{\langle q(ab)\alpha JM|V_{N-1,N}|q'(cd)\alpha' J'M'\rangle - \langle q(ab)\alpha JM|V_{N-1,N}|q'(dc)\alpha' J'M'\rangle\right\}. \quad (6.6)$$

The coupling schemes, indicated implicitly by α and α' for the initial and final states, respectively, have not been specified yet. The initial state is composed of closed shells with a vacancy in one of them and therefore has no term structure. The final state consists of two vacancies and one continuum electron. We consider the coupling scheme such that the two almost filled subshells A and B are first coupled to form an ion core specified by the total angular momentum J_{ab}. The core state is then coupled to the continuum orbital D. This coupling scheme of the final state is given explicitly as

$$\langle[(J_aJ_b)J_{ab}j_d]JM| \quad . \quad (6.7)$$

Now we proceed to evaluate the semisymmetrized matrix elements in (6.6) with the coupling scheme (6.7) for the final state.

Direct matrix element

For the first term in the curly brackets in (6.6), we obtain the following.

Step (ii)-(v): Because those subshells J_λ which neither involve coupling with other subshells nor contain active particles can be ignored, we obtain

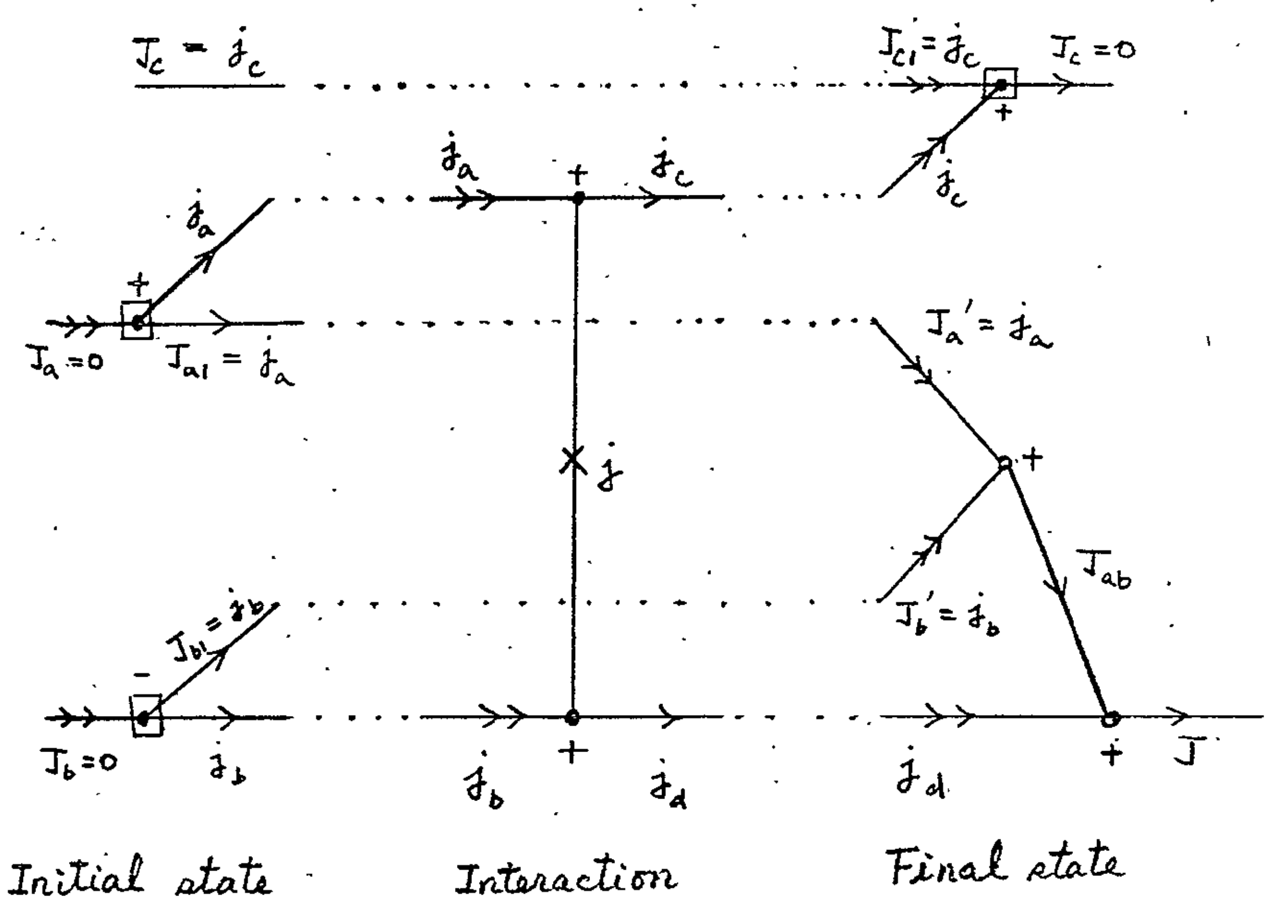

(6.8)

Here the interaction strength, denoted by the cross "X" in the interaction block, of the potential (6.2) can easily be looked up in Appendix B. Note that all the c.f.p. in the diagram (6.8) are trivially unity although we retain the c.f.p. symbols to illustrate the decouplings. Also we have made use of the simple relations (2.25) and (2.26) in decoupling closed shells.

Step (vi): The 3-jm representation of (6.8) is given as

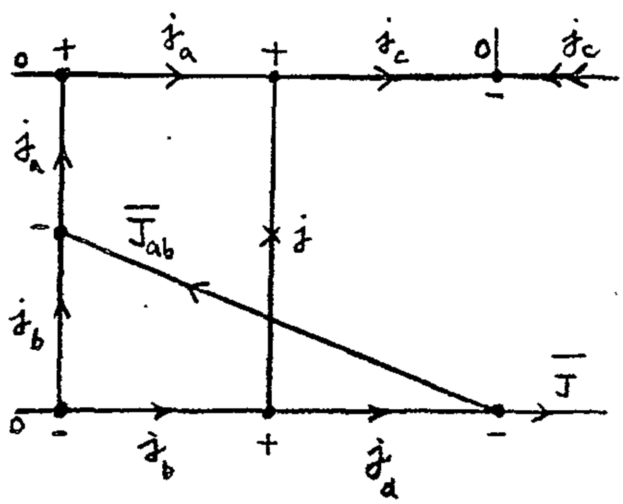

(6.9)

Step (vii): We use the transformation rule (2.11) to join the nonzero free angular-momentum lines j_c and J,

$\delta_{J j_c}\ \delta_{M m_c}$

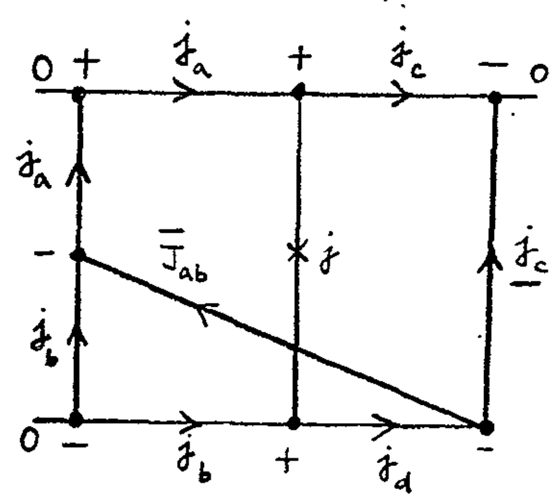

(6.10)

By applying the transformation rule (2.12) to the zero angular-momentum lines in (6.10), we obtain the simple diagram

$$\delta_{Jj_c}\,\delta_{Mm_c}$$

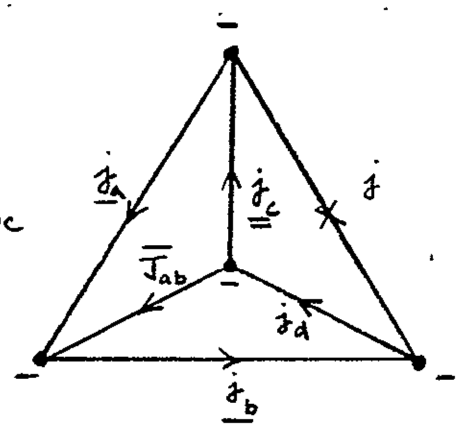

$$= \delta_{Jj_c}\,\delta_{Mm_c}\sum_{j} X_{j}(ab;cd)(2J_{ab}+1)^{1/2}$$

$$\left[(2j_a+1)(2j_b+1)(2j_c+1)^2\right]^{-1/2}$$

$$(-)^{2j_a+2j_b+2j_d}\begin{Bmatrix} j_a & j_b & J_{ab} \\ j_d & j_c & j \end{Bmatrix} .$$

(6.11)

Exchange matrix element

For the second term in the curly brackets in (6.6), we proceed as follows.

Step (ii)-(v):

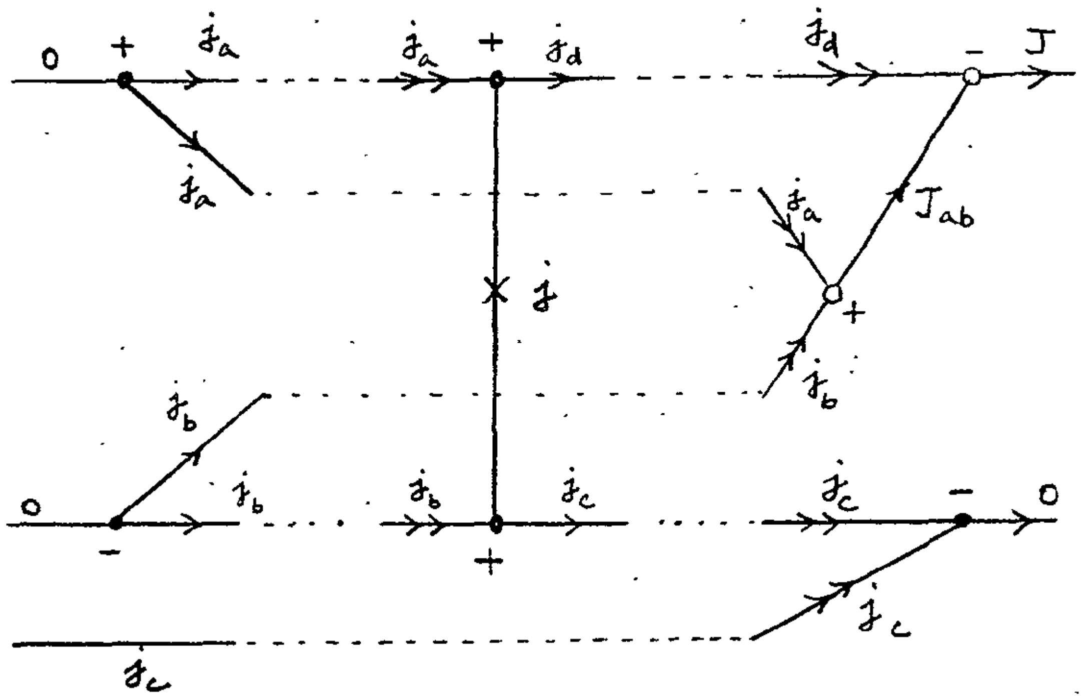

(6.12)

Step (vi):

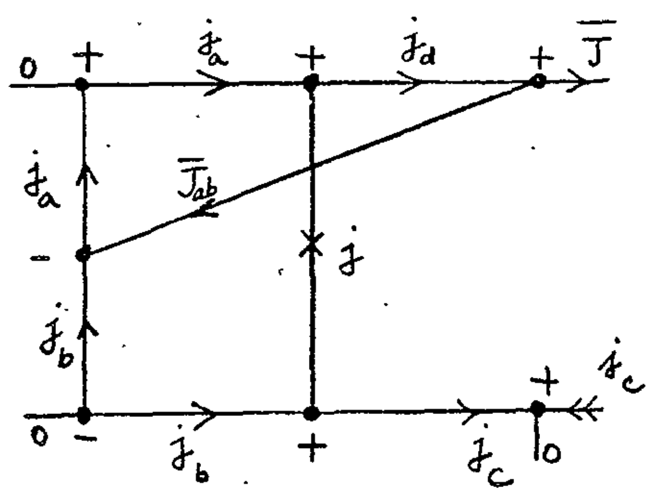

(6.13)

Step (vii):

$\delta_{Jj_c}\delta_{Mm_c}$ 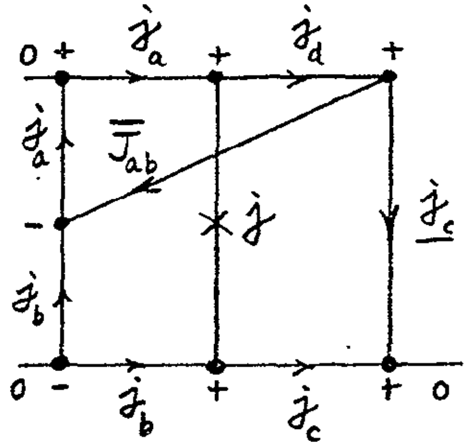

$=\ \delta_{Jj_c}\delta_{Mm_c}$ 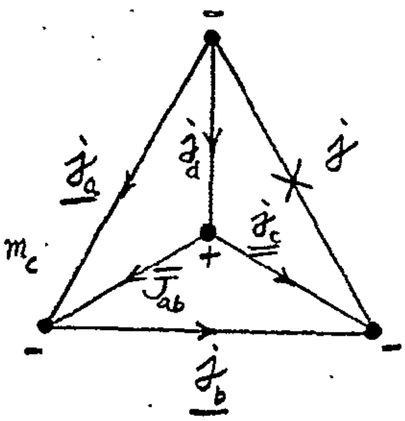

$$= \delta_{Jj_c}\delta_{Mm_c}\sum_{j} X_{j}(ab;dc)(2J_{ab}+1)^{1/2}$$
$$\times\left[(2j_a+1)(2j_b+1)(2j_c+1)^2\right]^{-1/2}(-)^{j_c-j_d-J_{ab}}\begin{Bmatrix} j_a & j_b & J_{ab} \\ j_c & j_d & j \end{Bmatrix}.$$

(6.14)

Step (viii): By substituting (6.11) and (6.14) into (6.3), we obtain the antisymmetrized matrix element (the transition amplitude) for the C-AB;D Auger transition in a singly ionized closed-shell atom,

$$T_{if}(C\text{-}AB;D) = \delta_{Jj_c}\,\delta_{Mm_c}\left(\frac{2J_{ab}+1}{2j_c+1}\right)^{1/2}\sum_{j}$$

$$\left[(-)^{j_c+j_d-J_{ab}} X_j(ab;cd)\begin{Bmatrix} j_a & j_b & J_{ab} \\ j_c & j_d & j \end{Bmatrix} - X_j(ab;dc)\begin{Bmatrix} j_a & j_b & J_{ab} \\ j_d & j_c & j \end{Bmatrix}\right]. \tag{6.15}$$

Here we have used the fact that j_a, j_b, j_c, and j_d are all half-integers to simplify the phase factor.

ACKNOWLEDGMENT

This work is supported in part by the U. S. Army Research Office (Grant DAHC04-75-G-0021) and by the National Aeronautics and Space Administration (Grant NGR 38-003-036) during the author's stay at the University of Oregon. The author would also like to thank Professor Anthony F. Starace for invaluable comments.

APPENDIX A: GLOSSARY OF TERMS

Clebsch-Gordan coefficient, Wigner coefficient

Alternative names for the vector-coupling coefficient.

Wigner 3-j coefficient or symbol

The symmetrized vector-coupling coefficient defined by Wigner (1951).

Covariant 3-jm coefficient or symbol

The vector-coupling coefficient defined in (2.2) in the covariant notation (Wigner, 1959).

3n-j coefficient or symbol

The 3-j symbol is defined as the triangular delta in (2.19). The 6-j and 9-j symbols have their usual meanings while the 12-j symbols and so on are not unique (Edmonds, 1957; Jucys et al., 1962; El-Baz and Castel, 1972).

3n-j coefficient or symbol of the first and second kind

The symmetrized recoupling coefficient defined by Levinson and Vanagas (1957). Their definitions are given in (2.22) and (2.23). (Jucys et al., 1962; El-Baz and Castel, 1972).

Subshell

A collection of particle states having the same quantum numbers n, ℓ, and j (or n and κ). (See, e.g., Grant, 1970.)

Configuration

A configuration is specified by the number of equivalent particles occupying each subshell and can be denoted by the aggregate $\{N_\lambda\}$.

Antisymmetrized many-particle state

The antisymmetrized state of a configuration. In this work, we mean exclusively the antisymmetrized jj-coupled state in which each subshell of equivalent particles is in a definite total subshell angular-momentum state and the whole many-particle system is in a definite grand total angular-momentum state.

Antisymmetrized matrix element

The matrix element between antisymmetrized many-particle states.

Semisymmetrized many-particle state

The many-particle state which is antisymmetric within each subshell but is not antisymmetric with respect to exchange of two particles from different subshells.

Semisymmetrized matrix element

The matrix element between semisymmetrized many-particle states.

Active particles

Those particles which actually participate in the interaction in a semisymmetrized matrix element.

Spectator particles

Those particles which, as opposed to active particles, do not participate in the interaction in a semisymmetrized matrix element.

jm-scheme matrix element

The matrix element between uncoupled Dirac single-particle orbitals.

Interaction graph

The geometric part of the jm-scheme matrix element of an interaction, which depends only on the tensorial properties of the interaction.

Interaction strength

The dynamical part of the jm-scheme matrix element of an interaction. It can be expressed in terms of reduced matrix elements of tensor operators involved in the interaction.

Bra and ket blocks

The diagram blocks representing the angular-momentum coupling of the bra and ket states, respectively, of the many-particle system.

Interaction block

The diagram block representing the jm-scheme matrix element of an interaction, including the interaction graph and the interaction strength.

Spectator block

The diagram block representing the scalar product of uncoupled spectator-particle states.

Recoupling diagram

The graphical representation of a recoupling coefficient.

APPENDIX B: GRAPHICAL FORMS OF OPERATORS AND POTENTIALS

In this appendix we will consider the jm-scheme matrix elements of one- and two-particle operators, i.e.,

$$\langle a | V^{(1)} | b \rangle \equiv \int d^3r\, U_a^{+} V^{(1)} U_b \,, \tag{B.1}$$

and

$$\langle ab | V^{(2)} | cd \rangle \equiv \int d^3r_1 \int d^3r_2\, U_a^{+}(1)\, U_b^{+}(2)\, V^{(2)} U_c(1)\, U_d(2) \,, \tag{B.2}$$

and their graphical representations. The Dirac orbitals in (B.1) and (B.2) are assumed to have the form

$$U_{n\kappa m} = \frac{1}{r} \begin{pmatrix} i\, G_{n\kappa}(r)\, \Omega_{\kappa m} \\ F_{n\kappa}(r)\, \Omega_{-\kappa m} \end{pmatrix} , \tag{B.3}$$

where the radial functions $G_{n\kappa}$ and $F_{n\kappa}$ are the large and small components, respectively, the $\Omega_{\kappa m}$ are normalized two-component Dirac spinors. Here the orbitals are completely specified by the quantum numbers n, κ, and m, which have their usual meanings (see, e.g., Grant, 1970). We will evaluate (B.1) and (B.2) in terms of radial integrals for various operators and potentials.

We first define various functions, notations, and coefficients and present a few useful formulas.

(i) Different combinations of radial wavefunctions:

$$W_{ab}(r) = G_a(r)\, G_b(r) + F_a(r)\, F_b(r) \ ,$$

$$Y_{ab}(r) = G_a(r)\, G_b(r) - F_a(r)\, F_b(r) \ ,$$

$$V_{ab}(r) = G_a(r)\, F_b(r) + F_a(r)\, G_b(r) \ ,$$

$$U_{ab}(r) = G_a(r)\, F_b(r) - F_a(r)\, G_b(r) \ ,$$

$$P_{ab}(r) = U_{ab}(r) + \frac{(\kappa_b - \kappa_a)}{j} V_{ab}(r) \ ,$$

$$Q_{ab}(r) = -U_{ab}(r) + \frac{(\kappa_b - \kappa_a)}{j+1} V_{ab}(r) \ . \tag{B.4}$$

(ii) Various radial functions:

$$R_\ell(r_1 r_2) = r_<^{\ell} / r_>^{\ell+1} \ , \tag{B.5}$$

where $r_<(r_>)$ is the smaller (larger) of r_1 and r_2.

$$g_\ell(r_1 r_2) = i\omega\, j_\ell(\omega r_<)\, h_\ell(\omega r_>) \ , \tag{B.6}$$

where j_ℓ and h_ℓ are the spherical Bessel and Hankel functions, respectively.

$$v_\ell(12) = \theta(r_1 - r_2)\left[R_{\ell+1}(r_1 r_2) - R_{\ell-1}(r_1 r_2)\right] \tag{B.7}$$

with $\theta(r_1 - r_2)$ the Heaviside step function

$$\theta(x) = \begin{cases} 1 & x \geq 0 \ , \\ 0 & x < 0 \ . \end{cases}$$

$$s_\ell(r_1 r_2) = \begin{cases} -\dfrac{i}{r_1}\, j_{\ell+1}(\omega r_2)\, h_\ell(\omega r_1), & r_1 > r_2 \,, \\[2ex] \dfrac{r_1^{\,\ell-1}}{\omega^2 r_2^{\,\ell+2}} - \dfrac{i}{r_1}\, j_\ell(\omega r_1)\, h_{\ell+1}(\omega r_2), & r_1 < r_2 \,. \end{cases}$$

(B.8)

$$t_\ell(r_1 r_2) = \begin{cases} \dfrac{r_2^{\,\ell-1}}{\omega^2 r_1^{\,\ell+2}} - \dfrac{i}{r_1}\, j_{\ell-1}(\omega r_2)\, h_\ell(\omega r_1), & r_1 > r_2 \,, \\[2ex] -\dfrac{i}{r_1}\, j_\ell(\omega r_1)\, h_{\ell-1}(\omega r_2), & r_1 < r_2 \,. \end{cases}$$

(B.9)

(iii) The following notations are used to denote integrals:

$$\langle f(r) \rangle = \int_0^\infty dr\, f(r) \,,$$

$$\langle P_{ab}(r_2)\, R_j(r_1 r_2) \rangle_2^{\text{even}} = \pi(l_a\, j\, l_b) \int_0^\infty dr_2\, P_{ab}(r_2)\, R_j(r_1 r_2) \,,$$

$$\langle P_{ac}(r_1)\, R_j(r_1 r_2)\, Q_{bd}(r_2) \rangle^{\text{even}} = \pi(l_a\, j\, l_c)\, \pi(l_b\, j\, l_d)$$

$$\times \int_0^\infty dr_1 \int_0^\infty dr_2\, P_{ac}(r_1)\, R_j(r_1 r_2)\, Q_{bd}(r_2) \,,$$

$$\langle P_{ac}(r_1)\, R_j(r_1 r_2)\, Q_{bd}(r_2) \rangle^{\text{odd}} = \pi(l_a\, j{+}1\, l_c)\, \pi(l_b\, j{+}1\, l_d)$$

$$\times \int_0^\infty dr_1 \int_0^\infty dr_2\, P_{dc}(r_1)\, R_j(r_1 r_2)\, Q_{bd}(r_2) \,,$$

where the parity selection function is defined as

$$\pi(l_a\, j\, l_b) = \begin{cases} 1 & \text{for } l_a + j + l_b \text{ even} \,, \\ 0 & \text{for } l_a + j + l_b \text{ odd} \,. \end{cases}$$

(iv) Define the coefficients

$$C_j(a;b) = (-)^{j_a+\frac{1}{2}}\left[(2j_a+1)(2j_b+1)\right]^{1/2}\begin{pmatrix} j_a & j & j_b \\ 1/2 & 0 & -1/2 \end{pmatrix},$$

(B.10)

$$C_j(ab;cd) = (-)^{j_a+j_d}\left[(2j_a+1)(2j_b+1)(2j_c+1)(2j_d+1)\right]^{1/2}$$

$$\times\begin{pmatrix} j_a & j & j_c \\ 1/2 & 0 & -1/2 \end{pmatrix}\begin{pmatrix} j_b & j & j_d \\ 1/2 & 0 & -1/2 \end{pmatrix}, \qquad \text{(B.11)}$$

$$C_{jm}(a;b) = \left(\frac{2j+1}{4\pi}\right)^{1/2} C_j(a;b)\begin{pmatrix} j_a & m & m_b \\ m_a & j & j_b \end{pmatrix}. \qquad \text{(B.12)}$$

(v)

$$I_j(K_a m_a, K_b m_b) = \int d\Omega\, \Omega^{+}_{K_a m_a} Y_{jm}\, \Omega_{K_b m_b}$$

$$= \pi(\ell_a j \ell_b)\, C_{jm}(a;b). \qquad \text{(B.13)}$$

(vi) The vector-spherical-harmonics expansion of $U_a^\dagger \vec{\alpha}\, U_b$:

$$U_a^\dagger \vec{\alpha}\, U_b = \frac{i}{r^2} \sum_{j\ell m} C_{jm}(a;b)\, \phi_{j\ell}(r)\, \vec{Y}_{j\ell m}(\hat{r}) \;, \tag{B.14}$$

where

$$\phi_{j(j-1)} = \pi(\ell_a j \ell_b)\,[j/(2j+1)]^{1/2}\, P_{ab}(r) \;,$$

$$\phi_{jj} = -\pi(\ell_a\, j+1\, \ell_b)\,[j(2j+1)]^{-1/2}\,(K_a+K_b)\, V_{ab}(r)$$

$$\phi_{j(j+1)} = \pi(\ell_a j \ell_b)\,[(j+1)/(2j+1)]^{1/2}\, Q_{ab}(r) \;. \tag{B.15}$$

This was first derived by Mann and Johnson (1971), and we have verified it independently. Since no derivation has previously been given for this extremely useful formula, we present its derivation in Appendix C. Many of the techniques of the vector-spherical-harmonics expansion may be found in various books (Rose, 1957; Edmonds, 1957; Akhiezer and Berestetskii, 1965).

(vii) The vector-spherical-harmonics expansion of $\vec{B}(1)$,

$$\vec{B}(1) = \vec{\nabla}_1 \int d^3 r_2 \, [U_b^+(2) \, \vec{\alpha}_2 \, U_d(2)] \cdot \vec{\nabla}_2 [(e^{i\omega r_{12}} - 1)/(\omega^2 r$$

is given as (Huang, 1978a)

$$\vec{B}(1) = i \sum_{j\ell m} C_{jm}(d;b) \, \psi_{j\ell}(r_1) \, \vec{Y}_{j\ell m}(\hat{r}_1), \tag{B.16}$$

where

$$\begin{aligned} \psi_{j(j-1)} &= [j/(2j+1)^3]^{1/2} \langle j \, g_{j-1} \, P_{bd}(r_2) \\ &\qquad - (j+1)[g_{j+1} + (2j+1) s_j] \, Q_{bd}(r_2) \rangle_2^{even} \\ \psi_{jj} &= 0 \\ \psi_{j(j+1)} &= [(j+1)/(2j+1)^3]^{1/2} \langle (j+1) \, g_{j+1} \, Q_{bd} \\ &\qquad - j[g_{j-1} + (2j+1) t_j] \, P_{bd} \rangle_2^{even} \end{aligned} \tag{B.17}$$

In the limit $\omega \to 0$, we have

$$\vec{B}(1) = -\frac{1}{2} \vec{\nabla}_1 \int d^3 r_2 \, U_b^+(2) \, \vec{\alpha} \, U_d(2) \cdot \vec{\nabla}_2 r_{12}$$

and the radial function $\psi_{j\ell}$ in (B.17) becomes

$$\psi_{j(j-1)} = j^{1/2} \left\langle \frac{j}{2j-1} R_{j-1} P_{bd}(r_2) - \frac{j+1}{2} v_j Q_{bd}(r_2) \right\rangle_2^{even}$$

$$\psi_{jj} = 0 ,$$

$$\psi_{j(j+1)} = (j+1)^{1/2} \left\langle \frac{j+1}{2j+3} R_{j+1} Q_{bd}(r_2) - \frac{j}{2} v_j P_{bd}(r_2) \right\rangle_2^{el}$$

(B.18)

One-particle Operator

We will present the jm-scheme matrix elements of the operator $f(r)$, β, $\vec{\alpha}\cdot\vec{p}$, $\vec{\alpha}$, $\vec{r}$, and $\vec{\alpha}\, e^{i\vec{k}\cdot\vec{r}}$ in turn.

$$\text{(i)}\ \langle a | f(r) | b \rangle = \delta_{\kappa_a \kappa_b} \delta_{m_a m_b} \langle W_{ab} f(r) \rangle$$

$$= \xrightarrow{j_a} \times \xrightarrow{j_b} , \qquad \text{(B.19)}$$

where the interaction strength, denoted by the cross "X" in (B.19), is

$$X(a;b) = \delta_{\ell_a \ell_b} \langle W_{ab} f(r) \rangle . \qquad \text{(B.20)}$$

Note that $\delta_{\kappa_a \kappa_b} \equiv \delta_{j_a j_b} \delta_{\ell_a \ell_b}$.

(ii)

$$\langle a|\beta|b\rangle = \xrightarrow{j_a} \ast \xrightarrow{j_b} \quad , \tag{B.21}$$

where

$$X(a;b) = \delta_{\ell_a \ell_b} \langle Y_{ab} \rangle . \tag{B.22}$$

(iii) The matrix element of $\vec{\alpha}\cdot\vec{p}$ may be obtained by making use of the formula

$$\langle a|\vec{\alpha}\cdot\vec{p}\,|b\rangle = -i\,\langle a|\vec{\alpha}\cdot\hat{r}\,|b'\rangle \tag{B.23}$$

with the understanding that $|b'\rangle$ denotes the Dirac orbital with the substitutions

$$\begin{aligned} G_b(r) &\longrightarrow G_{b'}(r) = \left(\frac{d}{dr} + \frac{K_b}{r}\right) G_b(r) \\ F_b(r) &\longrightarrow F_{b'}(r) = \left(\frac{d}{dr} - \frac{K_b}{r}\right) F_b(r) \end{aligned} \tag{B.24}$$

for the radial parts of the orbital $|b\rangle$. By using the expansion (B.14) and the formula

$$\int d\Omega\, \hat{r}\cdot \vec{Y}_{j\ell m} = -\sqrt{4\pi}\; \delta_{j0}\, \delta_{\ell 1}\, \delta_{m0} \quad , \tag{B.25}$$

we can easily obtain the result

$$\langle a|\vec{\alpha}\cdot\vec{p}\,|b\rangle = \delta_{K_a K_b}\, \delta_{m_a m_b} \langle U_{ab'} \rangle . \tag{B.26}$$

This agrees with the result obtained using other methods (see, e.g., Rose, 1957; Grant, 1970). Hence the graphical representation is

$$\langle a|\vec{\alpha}\cdot\vec{p}\,|b\rangle =$$ 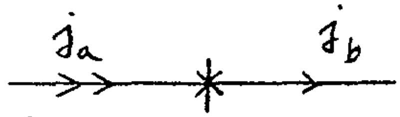

(B.27)

with the interaction strength

$$X(a;b) = \delta_{l_a l_b}\langle U_{ab'}\rangle . \tag{B.28}$$

(iv) By using the expansion (B.14) and the formula (B.13), we obtain

$$\langle a|\vec{\alpha}\,|b\rangle = \begin{pmatrix} j_a & 1 & m_b \\ m_a & m_b-m_a & j_b \end{pmatrix} C_1(a;b)\, I_1(a;b) , \tag{B.29}$$

where the radial integral is

$$I_1(a;b) = i\,\hat{e}_{m_b-m_a}\langle P_{ab}\rangle^{even} . \tag{B.30}$$

Here $\hat{e}_q$ is the spherical unit vector (Edmonds, 1957). Therefore its graphical representation is

$$\langle a|\vec{\alpha}\,|b\rangle =$$ 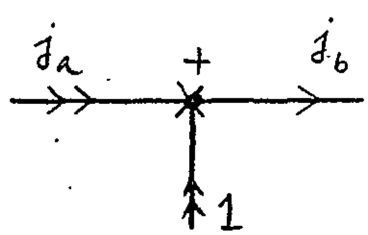

(B.31)

with the interaction strength

$$X_1(a;b) = C_1(a;b)\, I_1(a;b). \tag{B.32}$$

(v) For $\langle a|\vec{r}|b\rangle$ we obtain the same interaction diagram as (B.31) with the radial integral given by

$$I_1(a;b) = -\hat{e}_{m_b-m_a} \langle W_{ab}\, r \rangle^{even}. \tag{B.33}$$

(vi) For $\langle a|\vec{\alpha}\, e^{i\vec{k}\cdot\vec{r}}|b\rangle$ we use the expansion (B.14) and the familiar Rayleigh expansion of a plane wave,

$$e^{i\vec{k}\cdot\vec{r}} = 4\pi \sum_{\ell=0} i^{\ell} j_{\ell}(kr) \sum_{m=-\ell}^{\ell} Y^{*}_{\ell m}(\hat{r})\, Y_{\ell m}(\hat{k}). \tag{B.34}$$

The rest of the calculation is straightforward, and the result is

$$\langle a|\vec{\alpha}\, e^{i\vec{k}\cdot\vec{r}}|b\rangle = \sum_{\substack{j\ell \\ q}} G_{j\ell}(a;b)\, X_{j\ell}(a;b). \tag{B.35}$$

Here the interaction graph is

$$G_{j\ell}(a;b) = (2j+1)^{1/2} \begin{pmatrix} j_a & j & m_b \\ m_a & m_b-m_a & j_b \end{pmatrix} \begin{pmatrix} m_b-m_a & \ell & 1 \\ j & m_b-m_a-q & q \end{pmatrix}$$

=

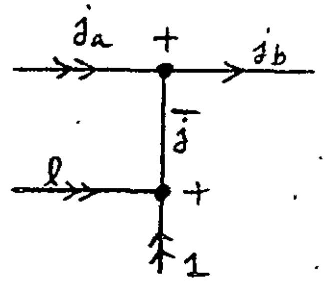

,

(B.36)

and the interaction strength is

$$X_{j\ell}(a;b) = \hat{e}_q C_j(a;b)(4\pi)^{1/2} i^{1-\ell} Y^{(\hat{k})}_{\ell(m_b-m_a-q)} D_{j\ell}$$

(B.37)

with $D_{j\ell}$ given as

$$D_{j\ell} = \begin{cases} -(j)^{1/2} < P_{ab}\, j_{j-1} >^{even}, & \ell = j-1, \\ (j)^{-1/2}(K_a + K_b)< V_{ab}\, j_j >^{odd}, & \ell = j, \\ -(j+1)^{1/2} < Q_{ab}\, j_{j+1} >^{even}, & \ell = j+1. \end{cases}$$

(B.38)

Two-particle Operator

We will deal only with rotational invariant interactions, which are generally linear combinations of zero-rank tensors obtained by contracting tensors of the same rank. The matrix element of these interactions can be calculated with the result (Huang, 1977, 1978a, and 1978b)

$$\langle ab|V(r_{12})|cd\rangle = \sum_j G_j(ab;cd) X_j(ab;cd),$$

(B.39)

where the interaction graph is

$$G_j(ab;cd) = \begin{pmatrix} j_a & j & m_c \\ m_a & m_c-m_a & j_c \end{pmatrix}\begin{pmatrix} j_b & m_d & m_c-m_a \\ m_b & j_d & j \end{pmatrix}$$

$$=$$

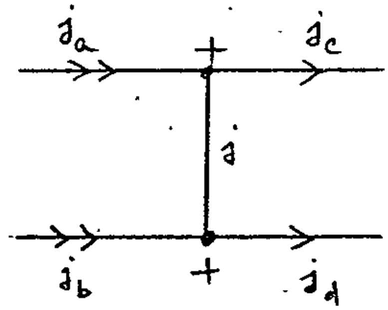

, (B.40)

and the interaction strength is

$$X_j(ab;cd) = C_j(ab;cd)\, I_j(ab;cd). \tag{B.41}$$

Here $I_j(ab;cd)$ is defined in terms of radial integrals, depending on the specific form of $V(r_{12})$. We summarize the results for various potentials:

(i) Coulomb potential: $\frac{1}{r_{12}}$

$$I_j(ab;cd) = \langle W_{ac} R_j W_{bd} \rangle^{even}. \tag{B.42}$$

(ii) Covariant photon interaction: $(1 - \vec{\alpha}_1 \cdot \vec{\alpha}_2)\ \frac{e^{i\omega r_{12}}}{r_{12}}$

$$I_j(ab;cd) = (2j+1)\langle W_{ac}\, g_j\, W_{bd}\rangle^{\text{even}}$$
$$- (1-\delta_{j0})(\kappa_a+\kappa_c)(\kappa_b+\kappa_d)\frac{2j+1}{j(j+1)}\langle V_{ac}\, g_j\, V_{bd}\rangle^{\text{odd}}$$
$$+ j\langle P_{ac}\, g_{j-1}\, P_{bd}\rangle^{\text{even}} + (j+1)\langle Q_{ac}\, g_{j+1}\, Q_{bd}\rangle^{\text{even}} .$$

(B.43)

This is obtained by using the expansion (B.14) and the formula

$$\int d\Omega_1\, d\Omega_2 \sum_{\nu=-\lambda}^{\lambda} Y^*_{\lambda\nu}(\hat{r}_1)\, Y_{\lambda\nu}(\hat{r}_2)\, \vec{Y}_{j\ell m}(\hat{r}_1)\cdot \vec{Y}_{j'\ell' m'}(\hat{r}_2)$$
$$= (-)^{j+\ell+m+1}\,\delta_{jj'}\,\delta_{\ell\ell'}\,\delta_{m(-m')}\,\delta_{\ell\lambda} . \qquad \text{(B.44)}$$

(iii) Transverse photon interaction:

$$-(\vec{\alpha}_1\cdot\vec{\alpha}_2)\frac{e^{i\omega r_{12}}}{r_{12}} + (\vec{\alpha}_1\cdot\vec{\nabla}_1)(\vec{\alpha}_2\cdot\vec{\nabla}_2)\left[\frac{e^{i\omega r_{12}}-1}{\omega^2 r_{12}}\right] .$$

$$I_j(ab;cd) = -(1-\delta_{j0})(\kappa_a+\kappa_c)(\kappa_b+\kappa_d)\frac{2j+1}{j(j+1)}\langle V_{ac}\, g_j\, V_{bd}\rangle^{\text{odd}}$$
$$+(\kappa_c-\kappa_a)\left[\langle V_{ac}\, g_{j-1}\, P_{bd}\rangle^{\text{even}} + \langle V_{ac}\, g_{j+1}\, Q_{bd}\rangle^{\text{even}}\right]$$
$$+j(j+1)\left[\langle P_{ac}\, s_j\, Q_{bd}\rangle^{\text{even}} + \langle Q_{ac}\, t_j\, P_{bd}\rangle^{\text{even}}\right] .$$

(B.45)

This is obtained by making use of the expansions (B.14) and (B.16) and the orthogonality relation

$$\int d\Omega_1 \vec{Y}^*_{j\ell m}(\hat{r}_1)\cdot\vec{Y}_{j'\ell' m'}(\hat{r}_1) = \delta_{jj'}\,\delta_{\ell\ell'}\,\delta_{mm'}\,. \tag{B.46}$$

(iv) Breit interaction:

$$-\frac{1}{2r_{12}}\left[(\vec{\alpha}_1\cdot\vec{\alpha}_2)+\frac{(\vec{\alpha}_1\cdot\vec{r}_{12})(\vec{\alpha}_2\cdot\vec{r}_{12})}{r_{12}^2}\right],$$

which represents the transverse photon interaction in the limit $\omega \to 0$.

$$\begin{aligned} I_j(ab;cd) = &-(1-\delta_{j0})(\kappa_a+\kappa_c)(\kappa_b+\kappa_d)\frac{1}{j(j+1)} \\ &+\frac{j(j+1)}{2j+1}\Big[\frac{1}{2j-1}\langle P_{ac}R_{j-1}P_{bd}\rangle^{even} \\ &+\frac{1}{2j+3}\langle Q_{ac}R_{j+1}Q_{bd}\rangle^{even} \\ &+\frac{1}{2}\langle Q_{ac}V_j(12)P_{bd}\rangle^{even}+\frac{1}{2}\langle P_{ac}V_j(21)Q_{bd}\rangle^{even}\Big]. \end{aligned} \tag{B.47}$$

(v) Operator $\vec{\alpha}_1 \cdot \vec{\alpha}_2$, which is proportional to the leading imaginary part of the transverse photon interaction.

$$I_j(ab;cd) = -\delta_{j1} \langle P_{ac} \rangle^{even} \langle P_{bd} \rangle^{even} . \tag{B.48}$$

APPENDIX C: VECTOR-SPHERICAL-HARMONICS EXPANSION OF $U_a^\dagger \vec{\alpha}\, U_b$

From the properties of the two-component Dirac spinor $\Omega_{\kappa m}$, we can easily prove that

$$\vec{\sigma}\cdot\hat{r}\,\Omega_{\kappa m} = -\Omega_{-\kappa m}\,,$$

$$\vec{\sigma}\cdot\vec{L}\,\Omega_{\kappa m} = -(\kappa+1)\,\Omega_{\kappa m}\,,$$

$$\vec{\sigma}\cdot i(\hat{r}\times\vec{L})\,\Omega_{\kappa m} = (\kappa+1)\,\Omega_{-\kappa m}\,. \tag{C.1}$$

Hence three useful formulas may be derived, i.e.,

$$\int d\Omega\,\Omega^{+}_{\kappa_a m_a}\vec{\sigma}\,\Omega_{-\kappa_b m_b}\cdot\hat{r}\,Y^{*}_{jm} = -I_j(\kappa_b m_b\cdot\kappa_a m_a)\,,$$

$$\int d\Omega\,\Omega^{+}_{\kappa_a m_a}\vec{\sigma}\,\Omega_{-\kappa_b m_b}\cdot\vec{L}\,Y^{*}_{jm} = -(\kappa_a+\kappa_b)\,I_j(-\kappa_b m_b\cdot\kappa_a m$$

$$\int d\Omega\,\Omega^{+}_{\kappa_a m_a}\vec{\sigma}\,\Omega_{-\kappa_b m_b}\cdot i(\hat{r}\times\vec{L})\,Y^{*}_{jm}$$

$$= (\kappa_b-\kappa_a)\,I_j(\kappa_b m_b\,,\,\kappa_a m_a)\,. \tag{C.2}$$

where $I_j(\kappa_b m_b, \kappa_a m_a)$, etc., are defined in (B.13). To obtain the vector-spherical-harmonics expansion of $U_a^\dagger \vec{\alpha}\, U_b$, i.e.,

$$U_a^{+} \vec{\alpha}\, U_b = \sum_{j\ell m} C_{j\ell m}(r)\, \vec{Y}_{j\ell m}(\hat{r}), \tag{C.3}$$

we simply evaluate the expansion coefficient as

$$C_{j\ell m}(r) = \int d\Omega\, U_a^{+} \vec{\alpha}\, U_b \cdot \vec{Y}^{*}_{j\ell m}(\hat{r}). \tag{C.4}$$

By using the formulars (C.2) and noting the relations

$$\vec{Y}_{j(j-1)m} = (2j+1)^{-1/2}\left[j^{1/2}\hat{r} - (j+1)^{1/2} i(\hat{r}\times\vec{L})\right] Y_{jm},$$

$$\vec{Y}_{jjm} = \left[j(j+1)\right]^{-1/2} \vec{L}\, Y_{jm},$$

$$\vec{Y}_{j(j+1)m} = (2j+1)^{-1/2}\left[-(j+1)^{1/2}\hat{r} - j^{1/2} i(\hat{r}\times\vec{L})\right]$$

and

$$\vec{\alpha} = \begin{pmatrix} 0 & \vec{\sigma} \\ \vec{\sigma} & 0 \end{pmatrix},$$

we can performs the angular integration of (C.4). The expansion (B.14) of $U_a^\dagger \vec{\alpha}\, U_b$ is thus obtained.

REFERENCES

Akhiezer, A. I. and V. B. Berestetskii, 1965, Quantum Electrodynamics (John Wiley, New York).

Auger, P., 1925, J. Phys. Radium 6, 205.

Bambynek, W., B. Crasemann, R. W. Fink, H.-U. Freund, H. Mark, C. D. Swift, R. E. Price, and P. V. Rao, 1972, Rev. Mod. Phys. 44, 716.

Bolotin, A., Y. Levinson, and V. Tolmacher, 1964, Licturos Fizikos Rinknigs 1, 33.

Bordarier, Y., 1970 (thesis, Univ. of Paris).

Briggs, J. S., 1971, Rev. Mod. Phys. 43, 189.

Brink, D. M. and G. R. Satchler, 1968, Angular Momentum (Oxford Univ. Press, Oxford), Chap. VII.

Condon, E. U. and G. H. Shortley, 1935, Theory of Atomic Spectra (Cambridge Univ. Press, Cambridge).

Danos, M., 1971, Ann. Phys. (N.Y.) 63, 319.

Dirac, P. A. M., 1930, The Principle of Quantum Mechanics (Clarendon Press, Oxford).

Eckart, C., 1930, Rev. Mod. Phys. 2, 235.

Edmonds, A. R., 1957, Angular Momentum in Quantum Mechanics (Princeton University, Princeton).

Edmonds, A. R. and B. H. Flowers, 1952, Proc. R. Soc. Lond. A 214, 515.

El-Baz, E., 1969, Traitement Graphique de L'Algebre des Moments Angulaires (Masson, Paris).

El-Baz, E. and B. Castel, 1971, Am. J. Phys. 39, 868.

El-Baz, E. and B. Castel, 1972, Graphical Methods of Spin Algebras in Atomic, Nuclear, and Particle Physics (Marcel Dekker, New York).

El-Baz, E. and S. Nahabetian, 1969, Nuovo Cimento Lett. 1, 583.

Fano, U., 1965, Phys. Rev. 140, A 67.

Fano, U. and G. Racah, 1959, Irreducible Tensorial Sets (Academic, New York).

Grant, I. P., 1970, Adv. Phys. 19, 747.

Grant, I. P., 1973, Comp. Phys. Commun. 5, 263.

Grant, I. P., 1976, Comp. Phys. Commun. 11, 397.

Harter, W. G. and C. W. Patterson, 1976, A Unitary Calculus for Electronic Orbitals (Springer-Verlag, Berlin).

Huang, K.-N., 1977, Phys. Lett. A 63, 262.

Huang, K.-N., 1978a, J. Phys. B.

Huang, K.-N., 1978b, Phys. Rev.

Huang, K.-N. and A. F. Starace, Phys. Rev.

The Institute of Atomic Energy, Academica Sinica, Tables of the Clebsch-Gordan Coefficients (Science Press, Peking, 1965).

Jucys, A. P. and A. A. Bandzaitis, 1967, Theory of Angular Momentum in Quantum Mechanics [in Russian] (Mintis, Vilnius).

Jucys, A. P., I. B. Levinson, and V. V. Vanagas, 1962, The Theory of Angular Momentum (Israel Program for Scientific Translation, Jerusalem).

Judd, B. R., 1963, Operator Techniques in Atomic Spectroscopy (McGraw-Hill, New York).

Judd, B. R., 1967, Second Quantization and Atomic Spectroscopy (Johns Hopkins, Baltimore).

Levinson, I. B. and V. V. Vanagas, 1957, Optika i Spektroskopiya 2, 10.

Mann, J. B. and W. R. Johnson, 1971, Phys. Rev. A 4, 41.

Massot, J.-N., E. El-Baz, and J. Lafoucrière, 1967, Rev. Mod. Phys. 39, 288.

Racah, G., 1942, Phys. Rev. 61, 186.

Racah, B., 1942, Phys. Rev. 62, 438.

Racah, G., 1943, Phys. Rev. 63, 367.

Rose, M. E., 1957, Elementary Theory of Angular Momentum (John Wiley, New Yor

Rotenberg, M., R. Bivins, N. Metropolis, and J. K. Wooten, Jr., 1959, The 3-j and 6-j Symbols (Technology, Cambridge, Mass.).

de-Shalit, A. and I. Talmi, 1963, Nuclear Shell Theory (Academic, New York).

Sivcev, V., A. Slepcov, I. Kickin, and Z. Rudzikas, 1974, Sov. Phys.-Coll. 14, 189.

Wigner, E. P., 1927, Z. Phys. 43, 624.

Wigner, E. P., 1951, "On matrices which reduce Kronecker products of representations of S. R. groups" (unpublished).

Wigner, E. P., 1959, Group Theory (Academic, New York), p. 295.